BRNO UNIVERSITY OF TECHNOLOGY
VYSOKÉ UČENÍ TECHNICKÉ V BRNĚ

FACULTY OF MECHANICAL ENGINEERING
ENERGY INSTITUTE

FAKULTA STROJNÍHO INŽENÝRSTVÍ
ENERGETICKÝ ÚSTAV

MATERIALS FOR IV. GENERATION POWER PLANTS

MATERIÁLY PRO JADERNÉ REAKTORY IV. GENERACE

BACHELOR'S THESIS
BAKALÁŘSKÁ PRÁCE

AUTHOR — MARTIN HOVORKA
AUTOR PRÁCE

SUPERVISOR — ING. LADISLAV ŠNAJDÁREK
VEDOUCÍ PRÁCE

BRNO 2014

Vysoké učení technické v Brně, Fakulta strojního inženýrství

Energetický ústav
Akademický rok: 2013/2014

ZADÁNÍ BAKALÁŘSKÉ PRÁCE

student(ka): Martin Hovorka

který/která studuje v **bakalářském studijním programu**

obor: **Strojní inženýrství (2301R016)**

Ředitel ústavu Vám v souladu se zákonem č.111/1998 o vysokých školách a se Studijním a zkušebním řádem VUT v Brně určuje následující téma bakalářské práce:

Materiály pro reaktory IV. generace

v anglickém jazyce:

Materials for IV. generation power plants

Stručná charakteristika problematiky úkolu:

Stručný popis konstrukce reaktorů IV. generace vzhledem k jednotlivým materiálovým požadavkům a to pro typy: VHTR, MSR a SCWR. Provést popis a srovnání současně dostupných kovových materiálů pro konstrukční prvek - přírubový spoj. Návrh experimentálního ověření pro náhradu ocelí novými typy a

Cíle bakalářské práce:

Stručný popis konstrukce reaktorů dle příslušných materiálových požadavků VHTR, MSR a SCWR.

Analýza současně dostupných kovových materiálů pro jeden konstrukční prvek - přírubový spoj.

Seznam odborné literatury:

BEČVÁŘ, Josef. Jaderné elektrárny. 2., opravené vyd. Praha: [s.n.], 1981, 634, [1] s. [4] s. obr. příl.

KONINGS, Rudy J. Comprehensive nuclear materials. Boston, MA: Elsevier, 2012. ISBN 978-008-0560-274.

ASM speciality handbook: Nickel, cobalt, and their alloys. Materials Park: ASM International, 2000. ISBN 978-0-87170-685-0.

databáze: www.sciencedirect.com, www.webofknowledge.com

Vedoucí bakalářské práce: Ing. Ladislav Šnajdárek

Termín odevzdání bakalářské práce je stanoven časovým plánem akademického roku 2013/2014.

V Brně, dne 22.11.2013

L.S.

doc. Ing. Zdeněk Skála, CSc. Ředitel ústavu	prof. RNDr. Miroslav Doupovec, CSc., dr. h. c. Děkan fakulty

ABSTRACT

The aim of this thesis is to describe material needs of chosen Generation IV nuclear reactors – VHTR, SCWR, and MSR with the emphasis on the VHTR. It describes the main principle and a constructional arrangement of VHTR components with its material demands. SCWR and MSR reactors are described in terms of its material requirements. The middle part of this thesis is dedicated to the available material candidate analysis. Main material properties are discussed and at the end of this part the suitability of chosen materials for a flange joint in VHTR heat exchanger is assessed.

The last chapter (the practical part) is focused on an experimental proposal of changeability of older materials by the new ones using the electron beam welding method.

KEYWORDS

Nuclear, reactor, IV generation, VHTR, material, SCWR, MSR, power plant, Monel, Inconel. Hastelloy.

ABSTRAKT

Cílem této práce je popis vybraných reaktorů IV. generace – VHTR, SCWR a MSR z hlediska jejich materiálových požadavků s důrazem na reaktor VHTR. V práci je popsán základní princip vysokoteplotního reaktoru a jeho základní uspořádání konstrukčních částí z hlediska materiálového namáhání. Ve střední pasáži jsou zanalyzovány 3 vybrané současně dostupné materiály. Jsou zde uvedeny zásadní vlastnosti daných materiálů a na konci této části je posouzena vhodnost jednotlivých typů ocelí pro použití v přírubovém spoji výměníku tepla vysokoteplotního reaktoru.

V poslední kapitole, v části praktické, je popsán návrh experimentálního ověření zaměnitelnosti a nahraditelnosti materiálů novými typy ocelí s použitím metody svařování elektronovým paprskem.

KLÍČOVÁ SLOVA

Jaderný, reaktor, IV. generace, VHTR, materiál, SCWR, MSR, jaderná elektrárna, Monel, Inconel, Hastelloy.

BIBLIOGRAPHIC CITATION

HOVORKA, M. *Materials for IV generation power plants.* Brno: Brno University of Technology, Faculty of Mechanical Engineering, 2014. 60 p. Supervisor Ing. Ladislav Šnajdárek.

DECLARATION

I declare that I have elaborated my bachelor's thesis on the topic of "Materials for IV generation power plants" independently, under the supervision of my supervisor Ing. Ladislav Šnajdárek and with the use of technical literature and other resources which are all quoted in this thesis and are specified in the list of literature at the end of the thesis.

Brno, May 30, 2014 ……..……

(author's signature)

ACKNOWLEDGEMENTS

I would like to express my thanks to Ing. Ladislav Šnajdárek for guiding this thesis and for many valuable insights and help. Moreover I would like to thank my parents for their loving support and encouragement.

CONTENTS

1. Introduction

Nuclear power plants provide approximately 16% of the electricity all around the globe but the future position of nuclear energetics in the present form is uncertain. Also there are still rumors about the lack of fluid hydrocarbons and there are the green-house effect global worries together with its impact to the environment. Right at this time the world is heading to the "politics of hydrogen". Hydrogen as an energy carrier can be used either as a transport fuel produced by electro-chemical reactions or for the production of drinkable water. A great amount of energy is necessary for the hydrogen production, which is why the new generation of power plants is being developed in recent years. This new generation could be used as a sufficient energy source for cogeneration of electricity and hydrogen production. Generation IV reactors are supposed to be technologically prepared around year 2030 with the exception of the VHTR reactor, which is expected to be prepared by the year 2021. The generation IV concept was proposed by the GIF organization (Generation IV International Forum) which determined 8 main points of interest. These points were represented by certain list of requirements considering the main improvements in which the new power plant generation has to be better than the older one. The requirements include for instance minimization of a nuclear waste, increase of efficiency of the power plant or improvement of nuclear safety.

There is a need to choose and investigate proper construction materials for the reactors, heat exchangers and other main components. It is necessary to guarantee that the generation IV reactors work with maximum safety, maximum stability, and proper efficiency. Due to enormous safety requirements for such a nuclear device, there is the necessity of knowing large amount of information about the structural materials to assure functionality of the system for a whole lifetime (which is approximately 60 years). By the present time there is a wide range of well-known materials. Many of them are tested and researched. The mainly tested materials are nickel-based alloy and composite materials.[1]

This thesis is divided into 2 parts. The theoretical one deals with the basic distribution, characteristics, and material requirements of 3 types of generation IV reactors such as VHTR, SCWR, and MSR with the main focus at Very High Temperature Reactor. Furthermore it deals with analyses of available nickel-based alloys and their properties such as creep rupture properties, tensile strength by the high temperatures, and corrosion resistance. The practical part deals with the discussion of suitability of electron beam welding of nickel-based alloys (specifically of Inconel 718). In addition there is a description of an experimental device proposal with simulated VHTR operating condition which could be used for testing changeability of new superalloys (nickel-based alloys) instead of older materials.

2. Generation IV reactors distribution

2.1. VHTR (Very High Temperature Reactor)

2.1.1. Basic information

A very high temperature reactor system is another level of development of gas-cooled reactors HTGR. The outlet temperatures are around 1000°C and even higher. There is chemically inert helium used as a coolant. VHTR system can produce hydrogen out of heat and water by the Iodine-Sulfur process or out of heat, water, and natural gas by methane reformation. It is expected that the hydrogen production unit with the rated power of 600MW_t could produce up to 2 million cubic meters of hydrogen per day. Due to high temperature the production of electric energy should be possible with the efficiency around 50% (compared with 47% of PBMR and GT-MHR with operating temperatures around 850°C). Cogeneration of heat and electricity production allows the VHTR work as a great heat source for refining or petrochemical industry. Figure 1 shows scheme of the cogeneration unit [2].

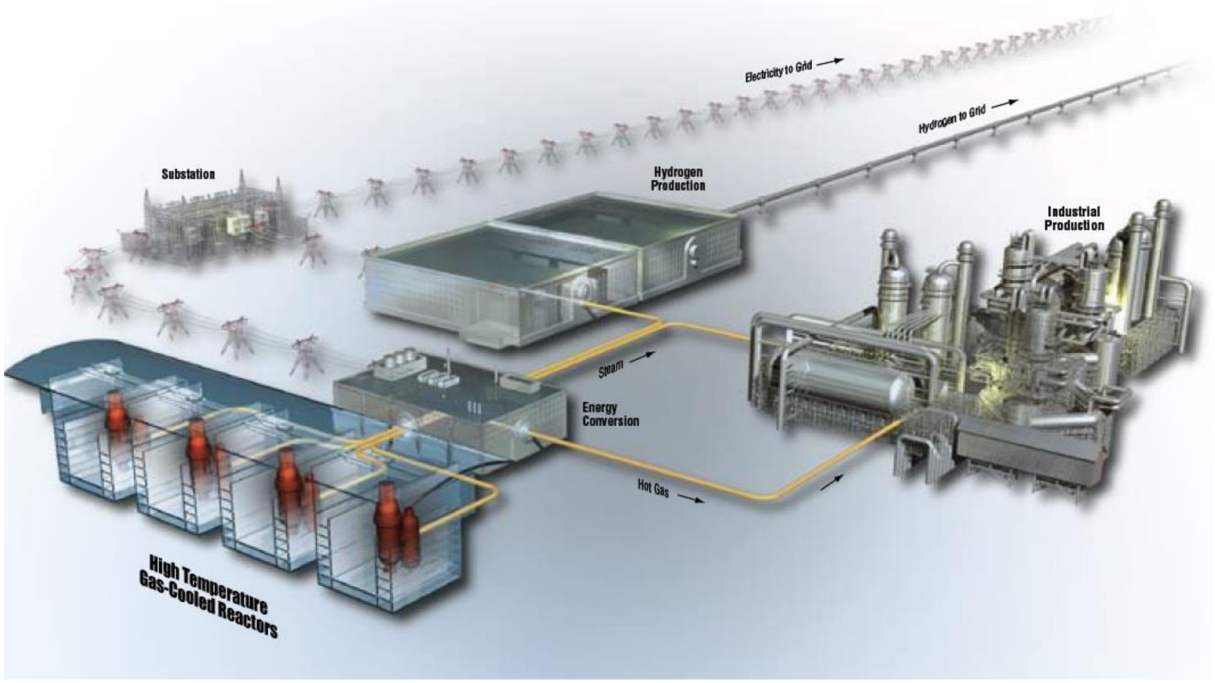

Figure 1: Scheme of cogeneration unit [3]

2.1.2. Reactor core

The reactor of VHTR nuclear power plant is still at the phase of final designing and development. In fact the proper core design has not been completely developed yet. There are 2 modification of the fuel assembly unit. Each fuel assembly modification includes proper portion of graphite moderator. Pebble-bed design, which was developed in Germany in early 80s, represents graphite balls with the diameter of 60mm. In each ball there is a cylindrical fuel pellet with the diameter of 20.4mm and height of 15.8mm (early conception). The second design modification is represented by prismatic hexagonal block developed by the United Kingdom and the United States during the Cold War. Both modifications are descripted in the following two subheads [4, 5].

2.1.2.1. Prismatic core design

The design is based on Generation III+ GT-MHR reactor designed by *General Atomics*. This form of core construction is a leading design candidate for the Korean project: *Nuclear Hydrogen Development and Demonstration.* Prismatic design consists of hexagonal fuel

assemblies (that are composed of fuel rods and moderator blocks) formed to an inner graphite reflector, a central active fuel core, and an outer replaceable graphite reflector. This composition is showed in the Figure 2. The active zone of the core is approximately 8 meters high and contains 102 fuel rods. Each rod is formed of 10 fuel blocks (there are 1020 fuel block in total). Apart from changeable graphite parts the prismatic core contains permanent side graphite reflector, cooling container channels and outer reactor casing [5].

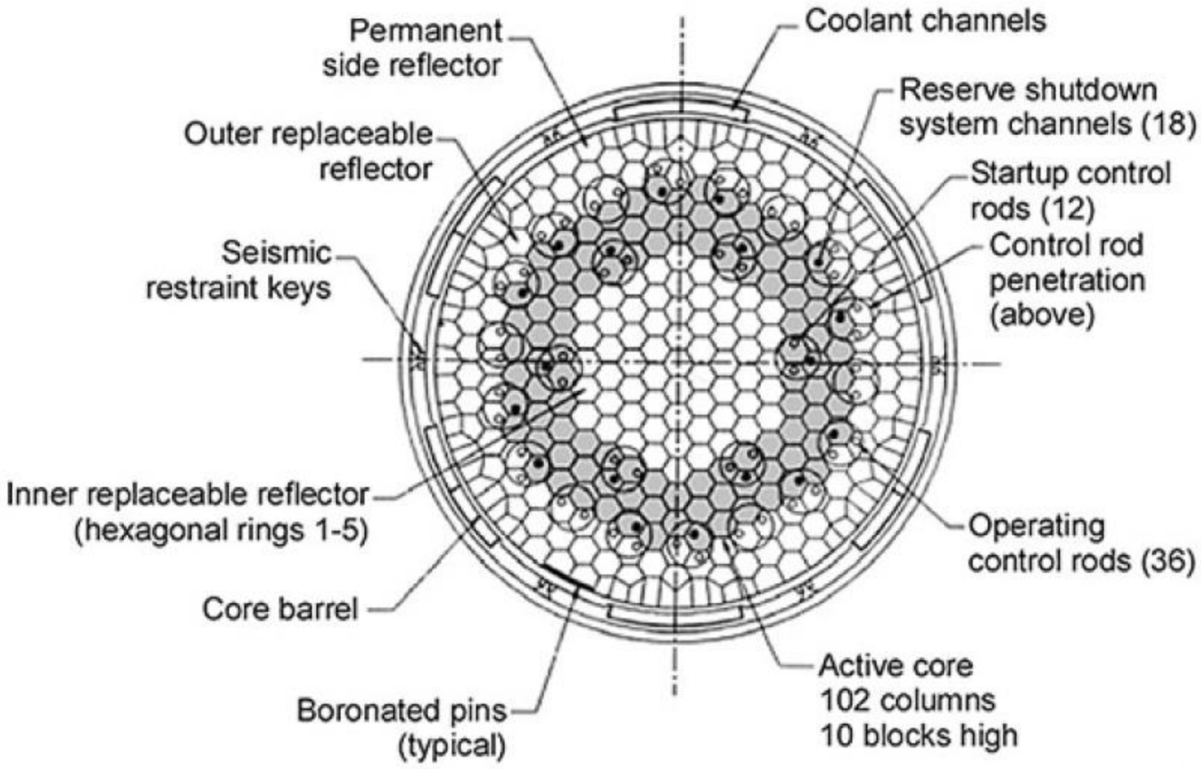

Figure 2: Prismatic core design [5]

Helium enters the core and flows up into the cooling container channels. After that it flows down through fuel assemblies cooling channel. This circulation enables the cooling of the outer casing and reduction of an operational temperature. For further imagination there is a cut of the prismatic core describing all construction parts of this design in the Figure 3.

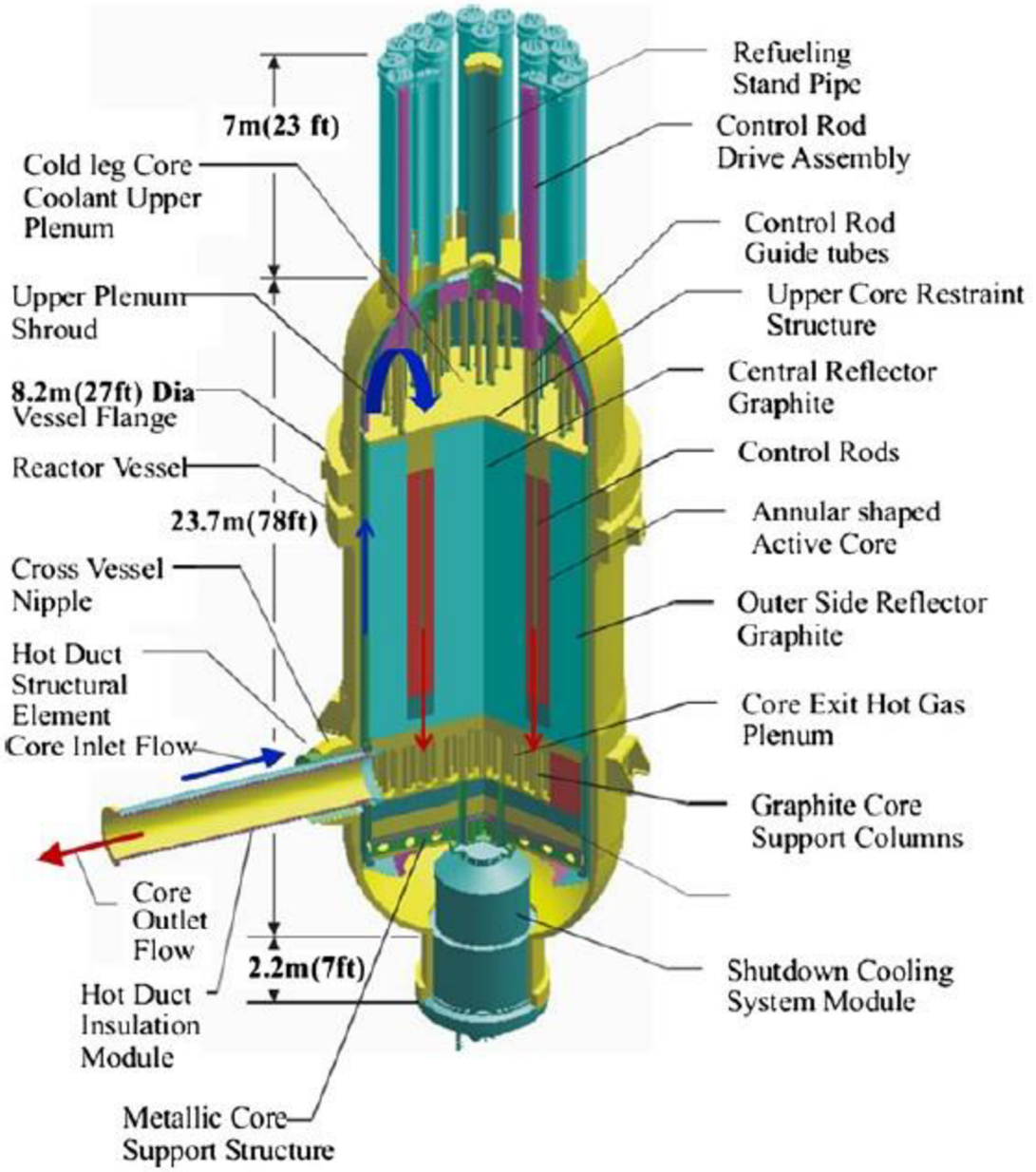

Figure 3: Prismatic core design cut [6]

In the Figure 4 there is a drawing of a VHTR prismatic core with further dimensions in millimeters and details. In the Figure 5 there is a detail of the hot gas duct as a drawing. It could be seen from the figure that the duct is formed of two sections. This structural duct separates the inlet gas flow from the core and the outlet gas flow to the core [7].

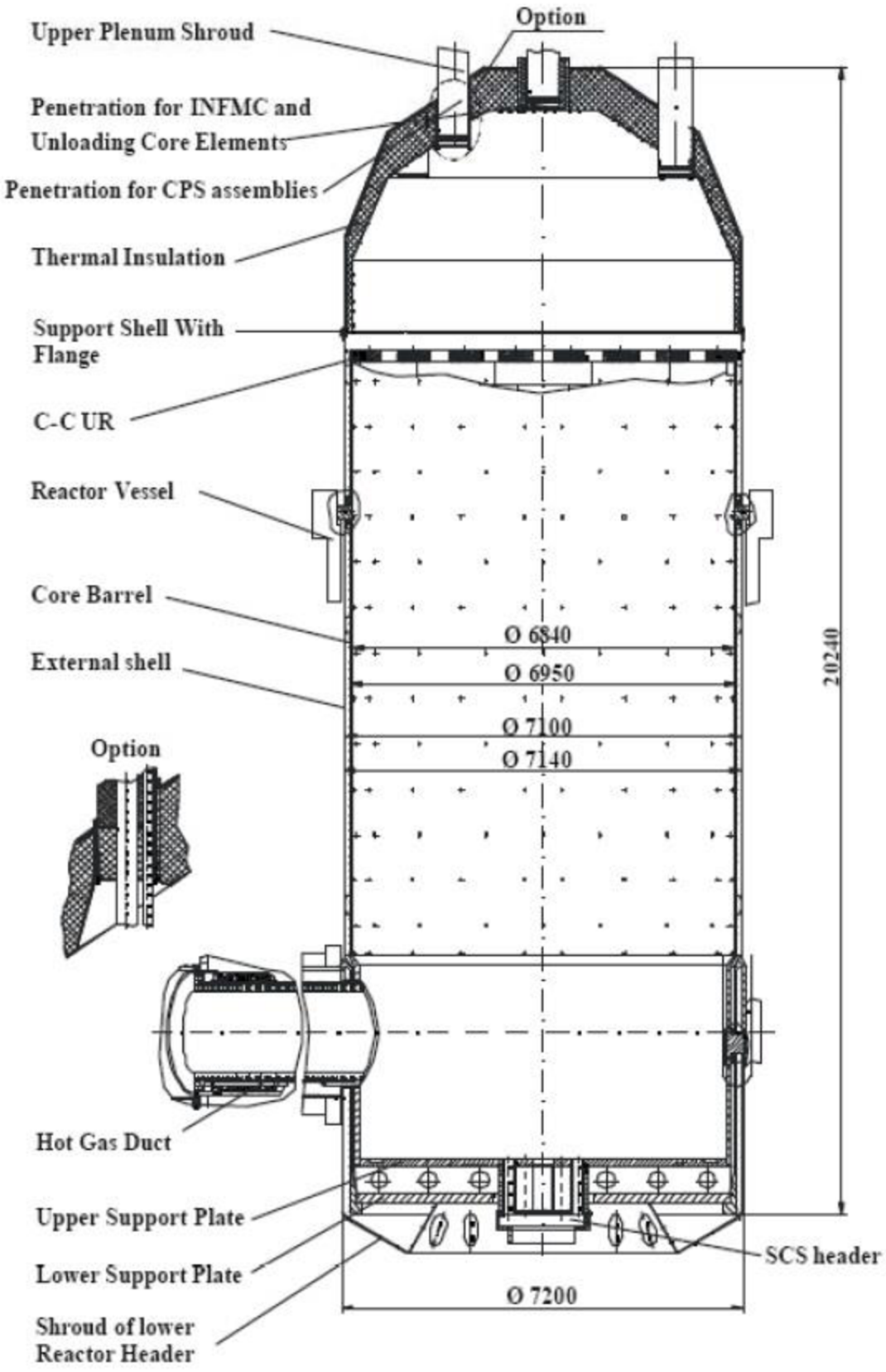

Figure 4: VHTR prismatic core drawing [7]

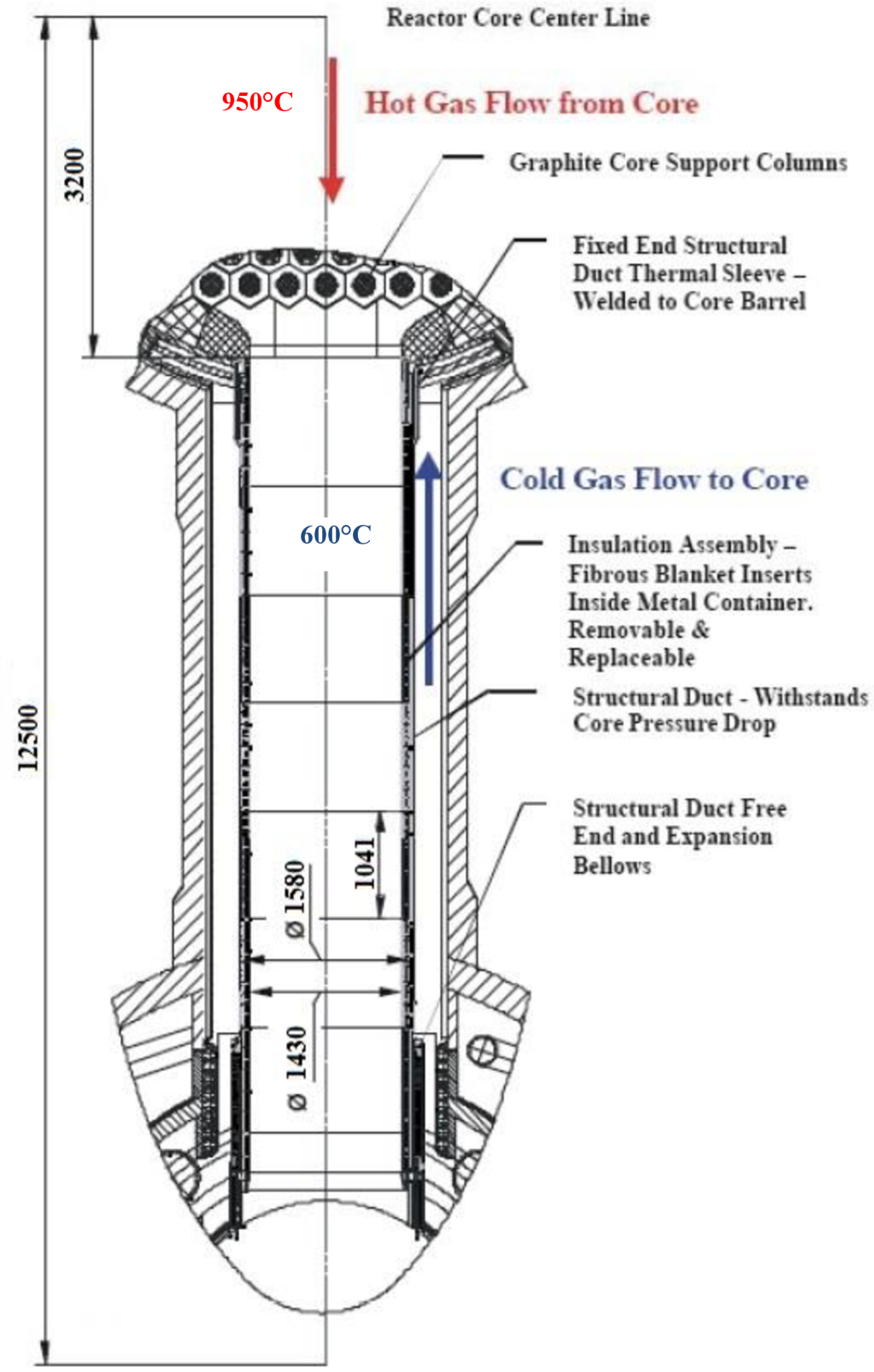

Figure 5: Hot gas duct drawing [7]

2.1.2.2. Pebble-bed core design

Pebble-bed design has its predecessor in Generation III+ PBMR reactor. This design is discussed in terms of Japanese first Very High Temperature systems. The arrangement of pebble-beds is similar to the prismatic design. Prismatic fuel blocks are replaced with mobile fuel balls of tennis ball size. These balls circulate down through the core continuously forced only by the gravity. At the end they are removed from the core, the burn rate is measured, and the active balls are returned back to the top of the reactor and a new circulation process begins. Inactive balls are transferred to storage. Inner and outer reflectors are built of a solid block of moderator similarly as the prismatic ones are. This form of construction enables easier fuel handling. But there is a necessity of changing the reflectors at least once per life cycle of the reactor. Pebble-bed reactors require external fuel manipulators for replacing and refilling of the fuel. This fact leads to increase of power plant construction costs and its operating time. With all these manipulators the online fuel handling is possible. Another system required is the system that controls and predicts the fuel pebble movements [5, 8].

There are also control rods included in both designs to regulation and stopping of a chain reaction. In the pebble-bed design there are additional small absorption balls to stop the nuclear fission and shutdown the reactor in emergency situations.

2.1.3. Power cycle

First generation of gas-cooled reactors with steam generators used an indirect Rankine cycle to produce electric energy. By that time the closed Brayton cycle was not completely discovered so main gas turbines used an open cycle. For the needs of nuclear energetics there was a necessity to close the cycle to prevent radioactive gas from diffusing. During the last decades of 20^{th} century the big progress in terms of development of closed Brayton cycle was achieved. Aircraft industry showed and proved high efficiency of the closed Brayton cycle. Moreover the closed Brayton cycle was much simpler than the indirect Rankine one. This fact led to many secure and economic advantages [5, 7].

VHTR will use the closed Brayton cycle for production of electricity because of advantages described above. For the production of hydrogen the VHTR will use the indirect cycle. There will be an intermediate heat exchanger (IHX) as a source of heat for the process.

The indirect cycle allows an isolation of the process heat loop of the nuclear reactor so that the process heat conduction net can be design as a net for non-nuclear usage. In addition the operating conditions as temperature, pressure, frequency, and thermal interface can vary from the conditions of the reactor core [5, 7].

2.1.4. Fuel and fuel system

Very high temperature reactors will use fuel developed in early 80s in Germany. It is a system developed on former generation of gas-cooled reactors. This fuel system is called TRISO which is a shortcut for Tristructural Isotropic. TRISO fuel is composed of elemental poppy seed sized particles. Each particle is ball shaped and contains uranium kernel coated with a carbon layer, a radiation-proof silicon carbide layer, and an outer carbon shell. The uranium core is made of low-enriched uranium oxycarbide (UCO). The ceramic layer is protected from chemical degradation of fission products by carbon layers. This ceramic layer loses its integrity at 1600 – 1800°C. Fuel elements are formed into the cylindrical wrapping of the size of a wooden pellet or a shotgun shell. One pellet contains approximately 96 000 fuel elements. VHTR system needs around 10^{10} of these elements. The position of single layers is displayed in Figure 6. In Figure 7 there is a picture of the fuel pellet in comparison to human hand [5, 9].

Thermal and irradiation stability of TRISO fuel element is designed with high expected safeness. Many measurements and experiments described in the literature and technical

articles show that the fuel particles can withstand temperatures up to 1600°C (as mentioned above) in fission operating environment. They are designed to avoid losing its integrity in emergency situations [10].

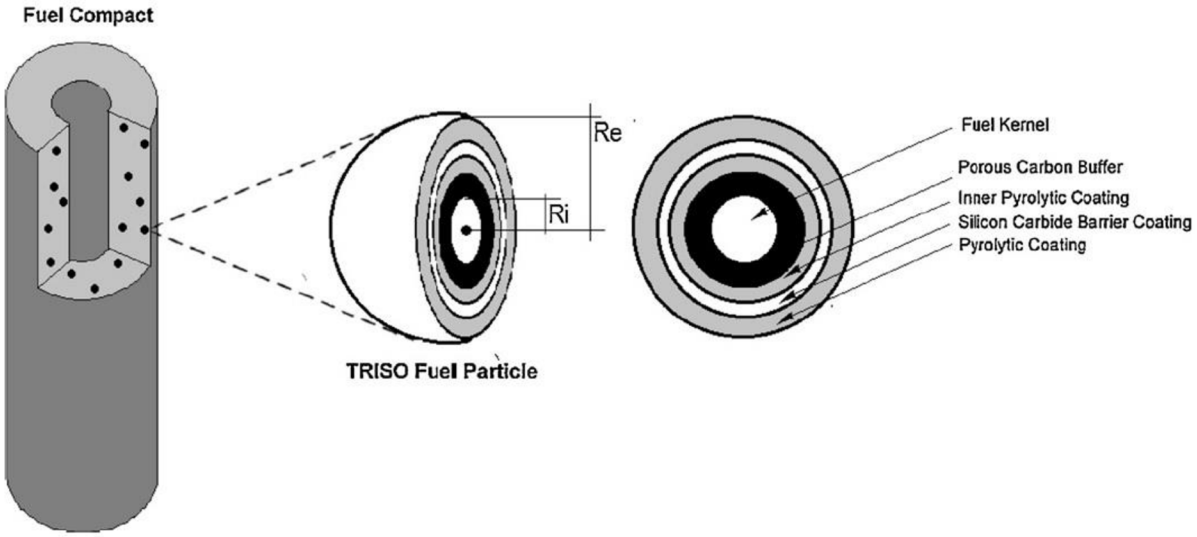

Figure 6: TRISO fuel element cut [11]

Where the fuel kernel radius R_i=425µm and the external graphite radius R_e=635µm.

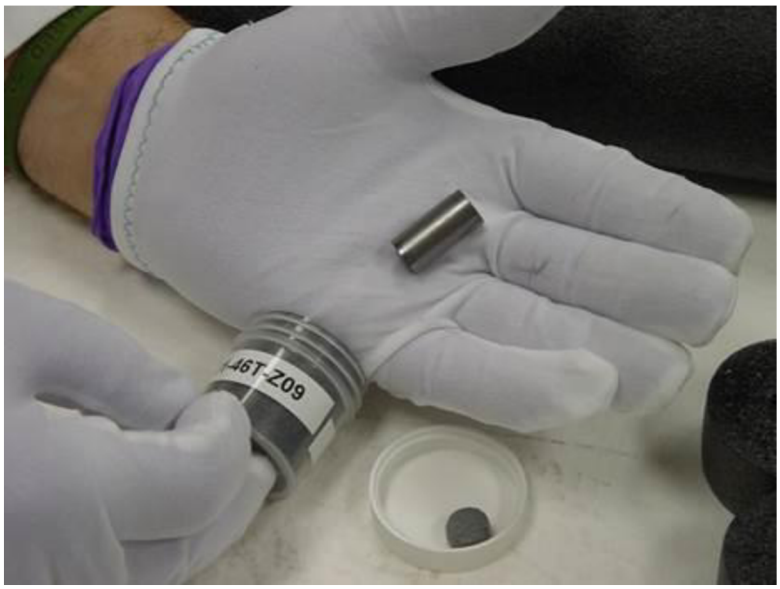

Figure 7: Fuel pellet (compact) [12]

Fuel pellets are formed into appropriate fuel blocks with a prismatic composition. More fuel blocks with an upper and a lower reflector form the fuel rod. The active part of the rod is around 8 meters high. The reflectors participate with 2 meters to final height. A standard fuel rod is made of 10 fuel blocks where each block includes 210 holes for the fuel pellets, and 108 influx outlets for the coolant. The major part of rods is made with the same configuration but some of them are made with emergency stop hole (channel) for regulation rods. Pebble-bed reactors use TRISO fuel blocks in a form of fuel balls. The fuel ball is made of many fuel elements coated in the graphite matrix. Process of the fuel block making is displayed in the Figure 8. The complete fuel rod model is showed in the Figure 9 [6, 9, 13].

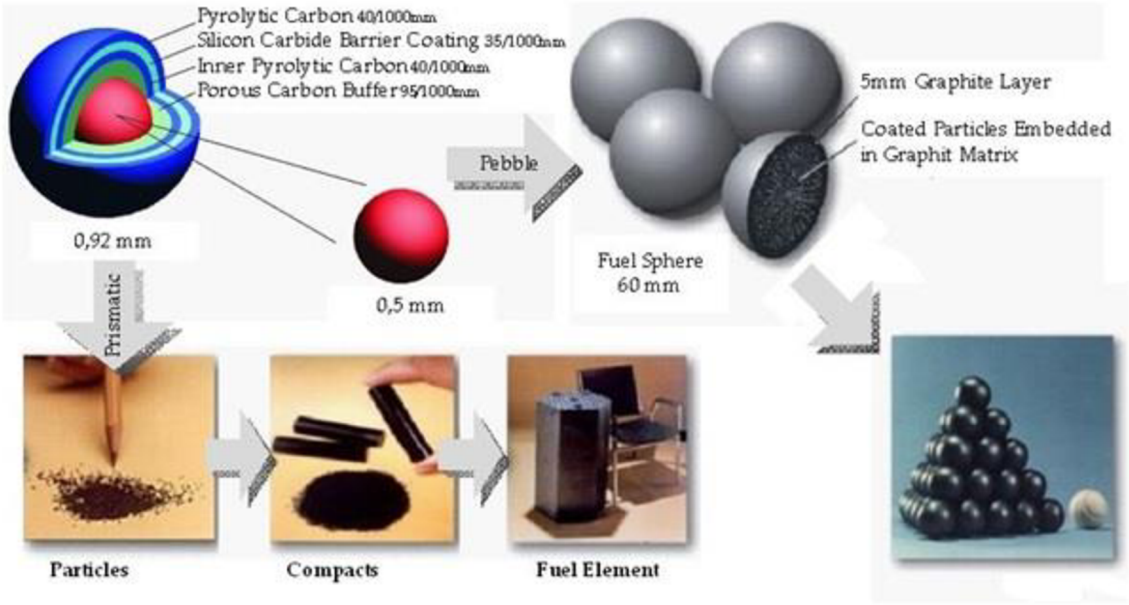

Figure 8: TRISO fuel manufacture [14]

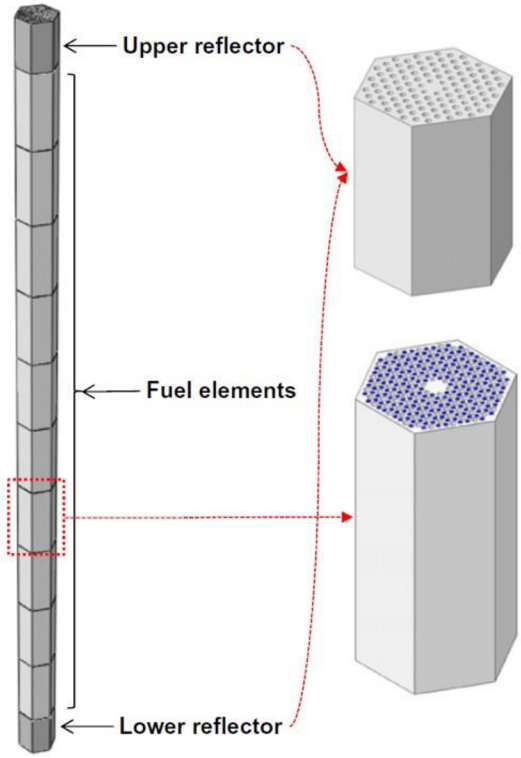

Figure 9: Fuel rod of Korean VHTR candidate (PMR600) [13]

2.1.4.1. Thermal-mechanical stress analysis of prismatic fuel rod [13]

Plenty of tests are made on experimental reactors to guarantee safety and functionality of nuclear reactors. But there are also many 3D numerical analyses made in CFD software for the evaluation of thermal and mechanical behavior. Proper material selection, selection of shapes of the construction structure, or an evaluation of limit states are accompanied by the necessity of knowing the pressures, strains and deformation caused by the core activity. CFD software is used to determine and predict different straining of critical reactor spots or straining around a whole reactor volume. The formation of a virtual model is required with the finite elements or finite volumes. Due to the symmetry of the fuel rod the model is just a part of examined structure (1/6 or 1/12). It is really convenient to use the object symmetry

because it has a huge impact on the number of solved equations. The less equations the numerical system has the more precise mesh can be generated. Precising of the finite-element mesh leads to more accurate results. Knowing that results from the finite element method and the finite volume method are just numerical results there is also the need to evaluate them critically and make an experiment, if possible.

Analysis chosen for this thesis is performed at a numerical model of 1/12 of the fuel rod which includes 17.5 holes for the fuel pellets, 8.5 standard outlets for coolant, and 0.5 small holes for control rod. This analysis evaluates an influence of a small gap between fuel rod body and the compact TRISO fuel block.

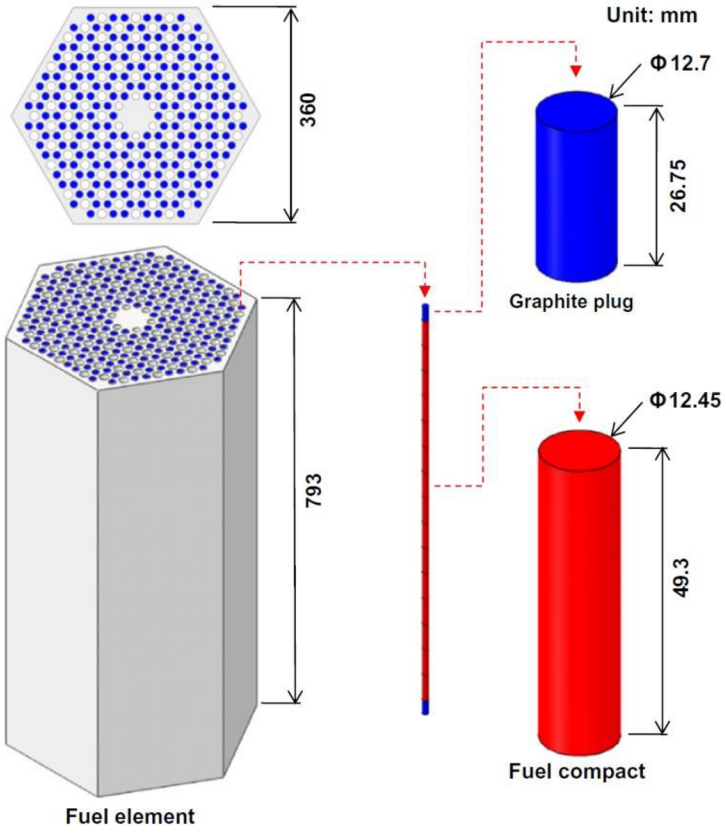

Figure 10: Evaluated fuel assembly of PMR600 [13]

First of all the numerical thermal analysis is performed at a linear model. The linear model does not include material characteristics and deformations between graphite regulator blocks and fuel blocks. Main purpose of this first step is to create a first insight into the problem and a thermal field for continuous mechanical part of the analysis as it is shown in Figure 11.

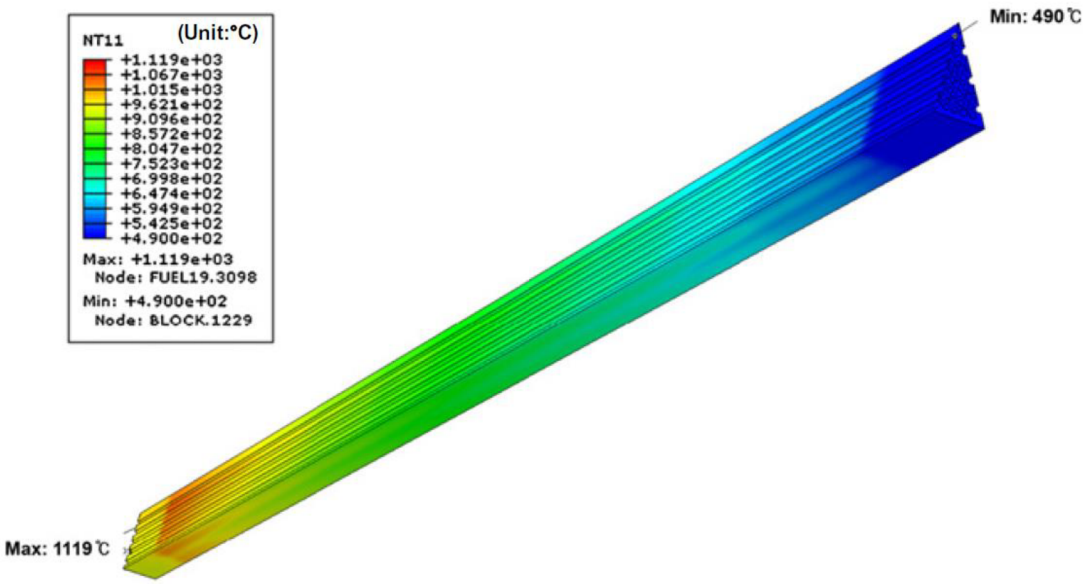

Figure 11: First step - Creation of thermal field [13]

After the first part of the calculation the material properties are assigned to the model. For this analysis the IG-100 material was used. The properties of IG-100 are recorded in the Table 1 below.

Because the thermal-mechanical analysis is non-linear, sub-models of the fuel rod have to be made. The new finite-element mesh with new boundary conditions is generated for each of those sub-models. Cutting the model into the sub-models makes this task solvable because degrees of freedom are greatly reduced. A scheme of the sub-modeling process is showed in the Figure 12.

Table 1: Material properties of IG-100 [13]

Properties	Symbols	Units	IG-100
Density	ρ	g/cm^3	1.78 (at 300K)
Young's modulus	E	GPa	$E=E_{20}(C_0+C_1T+C_2T^2+C_3T^3+C_4T^4+C_5T^5)$ E_{20}=7.9 C_0=1.0 C_1=1.3328e-5 C_2=-1.5281e-7 C_3=4.4335e-10 C_4=-2.5016e-13 C_5=4.8723e-17
Poisson's ratio	ν	-	0.14
Comprehensive strength	σ_c	MPa	76.9 (at 300K)
Tensile strength	σ_t	MPa	25.3 (at 300K)
Mean coefficient of thermal expansion	α	K^{-1}	$\alpha=\alpha_{400}(C_0+C_1T+C_2T^2)$ 100≤T [°C]≤1500 α_{400}=4.06e-6 C_0=0.853157 C_1=4.26564e-4 C_2=-1.42849e-7

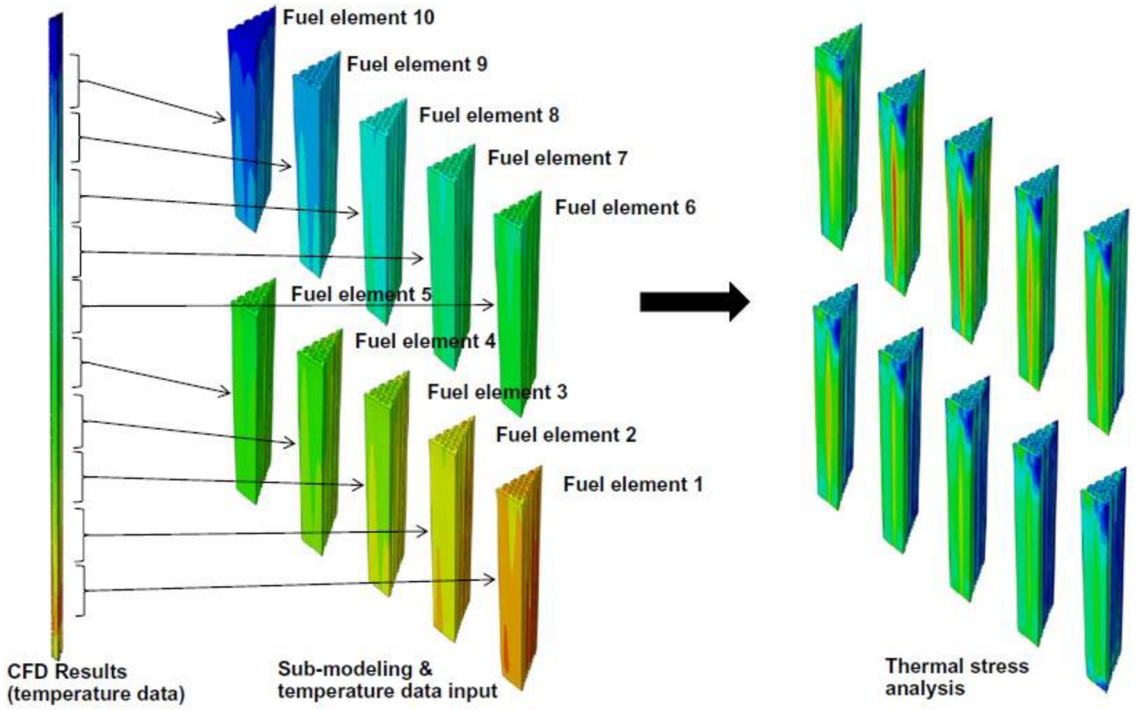

Figure 12: Sub-modeling procedure [13]

The generated mesh (Figure 13) is numerically solved and evaluated strains and stresses are displayed (Figure 14). Critical spots are chosen for further valorization of limit state of strength.

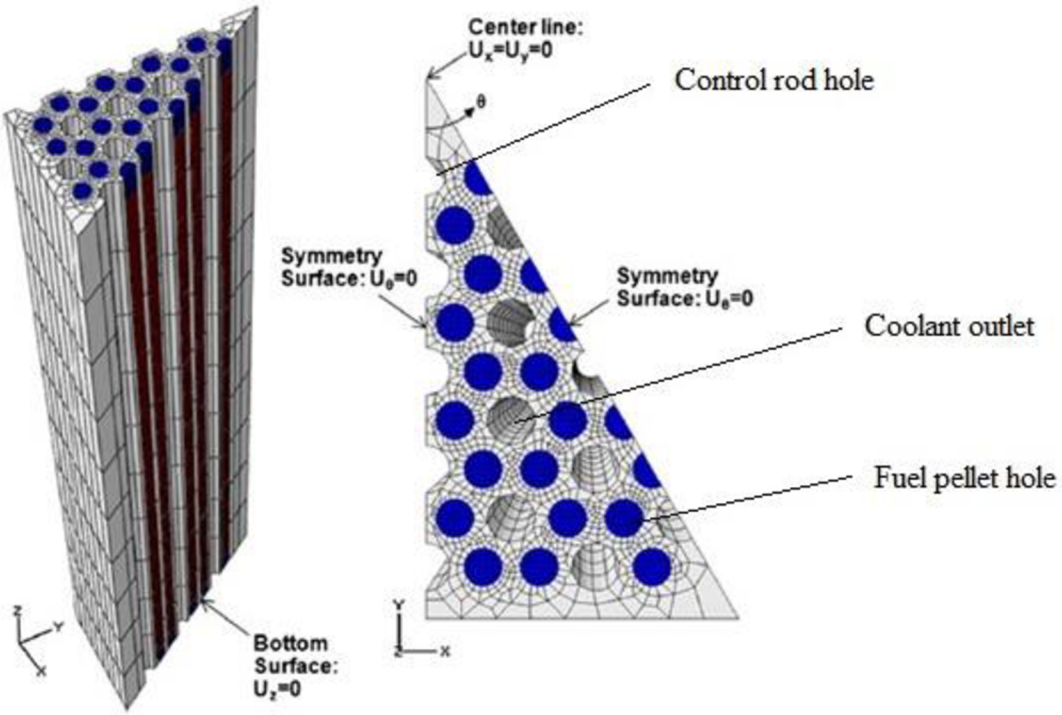

Figure 13: Generated finite-element mesh [13]

Majority of the contemplated materials for VHTR usage has the value of tensile strength around 90 MPa at 1000°C. The CFD simulation is performed on every single sub-model and a decrease of stress is found out at a critical spot between the graphite reflector plug and the fuel block (as is showed in the Figure 14). This analysis is following thermal-mechanical

solution for previous analysis performed by the scientists of *Korean Atomic Energy Research Institute* but unfortunately the previous one isn't currently available.

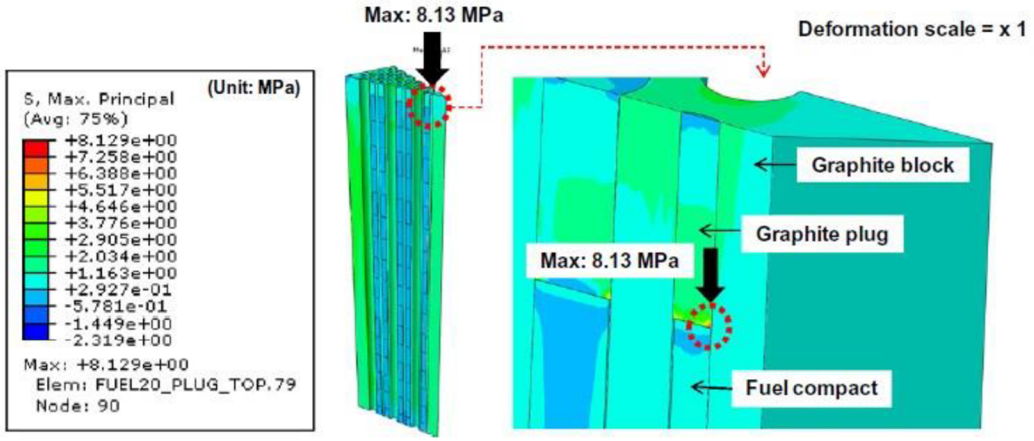

Figure 14: Maximum stress at 10th sub-model [13]

The main goal of this performance is to check an influence of the gap in the area described above. After the numerical solution is made, the evaluation of limit states begins. Except of the evaluation of limit states of strength at the area of the gap there are also places with the highest values of pressure evaluated. After all evaluations the stress and structural integrity is proven. The values of stresses lie in the interval of safety. And the influence of gap appears as indispensable in terms of stress and strain analysis.

CFD analyses are also suitable for evaluation of wide range of material properties and for verifying behavior and changeability of tested materials.

2.1.5. Material requirements

VHTR systems belong to the IV generation power plants capable of producing electricity with high efficiency and producing large amount of hydrogen. Structural materials of such reactor are exposed to very high temperatures, up to 1000°C, and much more intense neutron radiation than the older reactor generation. Nickel-based alloys are considered as materials which can withstand such a rough environment. There is a list of materials that meet the requirements for VHTR structural materials. Considered materials are for example: Inconel (230, 617, or 718) or Hastelloy (X, XR). Two subheads below are dedicated to Inconel 718 and Hastelloy X (XR). But even these superalloys, that is how the nickel-based alloys are named sometimes, subject to unstoppable aging and time degradation. However the VHTR final concept is still not completed so the demands on structural materials can vary through the time [5].

High core temperatures and the huge neutron flux lead to many interactions with irradiated surface, a lot of diffusion interactions, and a wide range of chemical reactions. These processes cause changes of the material microstructure which leads to changes of the material properties. An inventory of main material properties is listed below. Part of the microstructure change research investigates influences of thermal and neutron effects by direct testing and numerical modelling. Because the microstructure changing processes are complex the empirical attitude is required. Gained results are used for creation respectively expansion of a material property and high-temperature behavior database in conditions close to the VHTR one [5, 15].

There was an idea to create a list of suitable materials that could withstand extreme conditions as high temperature or irradiation. First of all, the list served as a material inventory for gas turbine construction for an aircraft industry. Later it was extended for nuclear reactors usage (especially for gas-cooled reactors). This register was formed for over 60 years. The list was published by *Kenneth Mills* in form of a book called *"Recommended values of*

thermophysical properties for selected commercial alloys" in 2002 (reference [15]). Of course, this was not the only published version of the inventory. Mills' issue contained various types of materials with its properties.

There is a necessity of showing and proving the safeness and suitability of each material for nuclear usage. After detailed research of gained material data there is an additional experiment to obtain specific properties of considered suitable material candidates. The information is enlisted into the database with declaration that it can be used in the environment of high temperatures and neutron flux. Also the service life has to be declared in the specific environments. Among compulsory recorded properties belong [5, 15]:

- Thermal expansion
- Heat capacity
- Irradiation growth
- Grain boundary growth
- Thermal creep
- Radiation creep
- Strength
- Ductility
- Toughness
- Creep rupture strength
- Fatigue cracking resistance
- Corrosion resistance
- Thermal diffusivity and conductivity
- Viscosity
- Density

Helium coolant inevitably contains certain amount of impurities. These impurities react along with water, hydrogen, and carbon in the reactor core and together they form the carbon monoxide and methane. The impurities reactions have influence on many chemical reactions in the whole reactor volume especially on the material surface. And the reactor temperature over 900°C accelerates these reactions significantly. This is another challenge that the materials have to overcome to guarantee a long-term service of the reactor.

Stable oxidation on the surface creates a thin protective layer that prevents the surface from outside degradation. However due to this layer a process of spallation can have an inauspicious effect on the integrity of material surface. On the other hand inner oxidation (inside the material) causes a reduction of the mechanical resistance while carburation causes an embrittlement and decarburation causes a reduction of material strength.

2.1.5.1. Material requirements of specific VHTR components

There are many demands required for every single construction component to meet with. The reactor core is mostly made of graphite elements such are the fuel parts, the reflectors, or core supports. For imagination of different thermal conditions and lifetime demands, there is the Table 2 filled with operating environmental conditions and demanded service time.

Considered materials for reactor internals are mainly nickel-based alloys and C/C composites (C/C stands for Carbon fiber-reinforced carbon). The VHTR internal operating conditions are shown in the Table 3 with material candidates for each structural part except the hot gas duct. The hot gas duct data are displayed in the Table 4.

Proper pressure vessel material is chosen as a compromise between certain warranted safety and suitable prize. Even if the outlet helium temperature reaches up to 1000°C the surface temperature of the vessel material is lower due to the cold helium entering straight to the wall of the vessel. Body temperature of the vessel can be regulated by the change of vessel dimensions, by density of the reactor performance, or by rated power of the reactor. Every change of the dimensions or operating conditions of the reactor has a quite big effect on operating costs and total budget. This is why there is a need of finding compromises that are economically allowable and the warranted safety is guaranteed. Present material candidates contain about 9% of chrome which prevents material from high temperature creep [5, 16].

Table 2: VHTR graphite component conditions [7]

VHTR Component	Normal Temperature [°C]	Abnormal Temperature [°C]	Pressure [MPa]	Fluence [n/cm^2]	Service time [yr]
Fuel Element block	600 to 1250	1600	5	$2.7 \cdot 10^{21}$	2.8
Replaceable reflectors	1100	1600	5	$2.7 \cdot 10^{21}$	15
Permanent side/lower reflectors	600/1100	1200	5	$2.0 \cdot 10^{20}$	60
Core support assembly	1000	1000	5	$5.0 \cdot 10^{18}$	60

Table 3: VHTR internal component conditions [7]

VHTR Component	Normal Temperature [°C]	Abnormal Temperature [°C]	Pressure [MPa]	Fluence [n/cm^2]	Service time [yr]	Material candidates
Core barrel or bottom plate and supports	600	700	5	$1.0 \cdot 10^{19}$	60	Incoloy 800
Upper plenum shroud	600	1200	5	$1.0 \cdot 10^{19}$	60	C/C composites + ceramic fibers
Operating control rod	1100	1600	5	$4.3 \cdot 10^{21}$	30	C/C + SiC/SiC composites

Because of high temperatures the proper materials for reactor's regulation parts and parts of the coolant system have to be researched intensely. Considered parts for regulation and coolant circuit are for example: regulation rods, hot gas pipeline, or closing (insulation) valves. Oxidation-reinforced nickel based alloys can meet with the condition for high temperature usage at temperatures around 1100°C but these alloys are relatively expensive. Molybdenum or tungsten based refractory alloys seem to be suitable for the high-temperature environment but there is a problem with their oxidation resistance. Superplastic ceramics are considered next but a further connection method research is required. Massive neutron flux inside the core makes the usage of metal material quite impossible. The regulation rods material is chosen of carbon composites and carbon fiber materials [5, 16].

Structural parts of the secondary power system also belong among the VHTR components. They are not that much influenced by neutron flux (but the high temperature remains) as the primary parts are and some of them are designed with lower lifetime demands. But it is desirable that these components work with same reliability as the primary ones. In the Table 5 there are shown parts of the power conversion system with its conditions and candidate materials.

Table 4: VHTR hot gas duct conditions [7]

Hot gas duct part	Normal Temperature [°C]	Abnormal Temperature [°C]	Pressure [MPa]	Fluence [n/cm^2]	Service time [yr]	Material candidates
Pressure bearing shell	600	660	5	$2.0 \cdot 10^{17}$	60	Incoloy 800
Outer shell of insulation element	950	980	5	$2.0 \cdot 10^{17}$	60	C/C composites
Thermal insulation	600-950	1000	5	$2.0 \cdot 10^{17}$	30	Mix of Al_2O_3-SiO_2 ceramic fiber

Table 5: VHTR power cycle component conditions [7]

VHTR Component	Normal Temperature [°C]	Abnormal Temperature [°C]	Pressure [MPa]	Fluence [n/cm^2]	Service time [yr]	Material candidates
Turbine inlet shroud	950	1000	5	$5.0 \cdot 10^{13}$	7	Inconel 617 or C/C composites
Turbine disks and blades	950	1000	5	$5.0 \cdot 10^{13}$	7	Ni-based alloys and DS Ni-based alloys or single crystals for blades
Recuperator	600	<600	5	$2.0 \cdot 10^{15}$	60	300 series stainless steel

Last but not least it is important to mention the research of protective layers of structural materials. These protective layers are formed of thin welded material covers. These welds are used wherever the material is extremely stressed or wherever the material cannot be made with proper constructional suitability. For example in IHX the welds are used for better flux shielding in hydrogen production.

2.2. SCWR (Supercritical Water Reactor)

2.2.1. Basic information

Supercritical water reactor systems are high-temperature water cooled systems operated by the critical point of water (which is at 374°C and 22.1 MPa). These systems have both, thermal and fast spectrum depended on a structural design of an active zone. SCWR reactors' efficiency reaches up to 44% (compared to LWR reactors: 33-35%). The SCWR conditions in comparison to LWR and PWR are shown in the T-S diagram in the Figure 15. Greater thermal amount of coolant allows reduction of size of main circulation pumps and its pipelines and a pump work. Because of the supercritical water condition there is no boiling crisis and there is a possibility of avoiding the construction components such are steam separators, steam dryers, steam generators, and recirculation pumps.

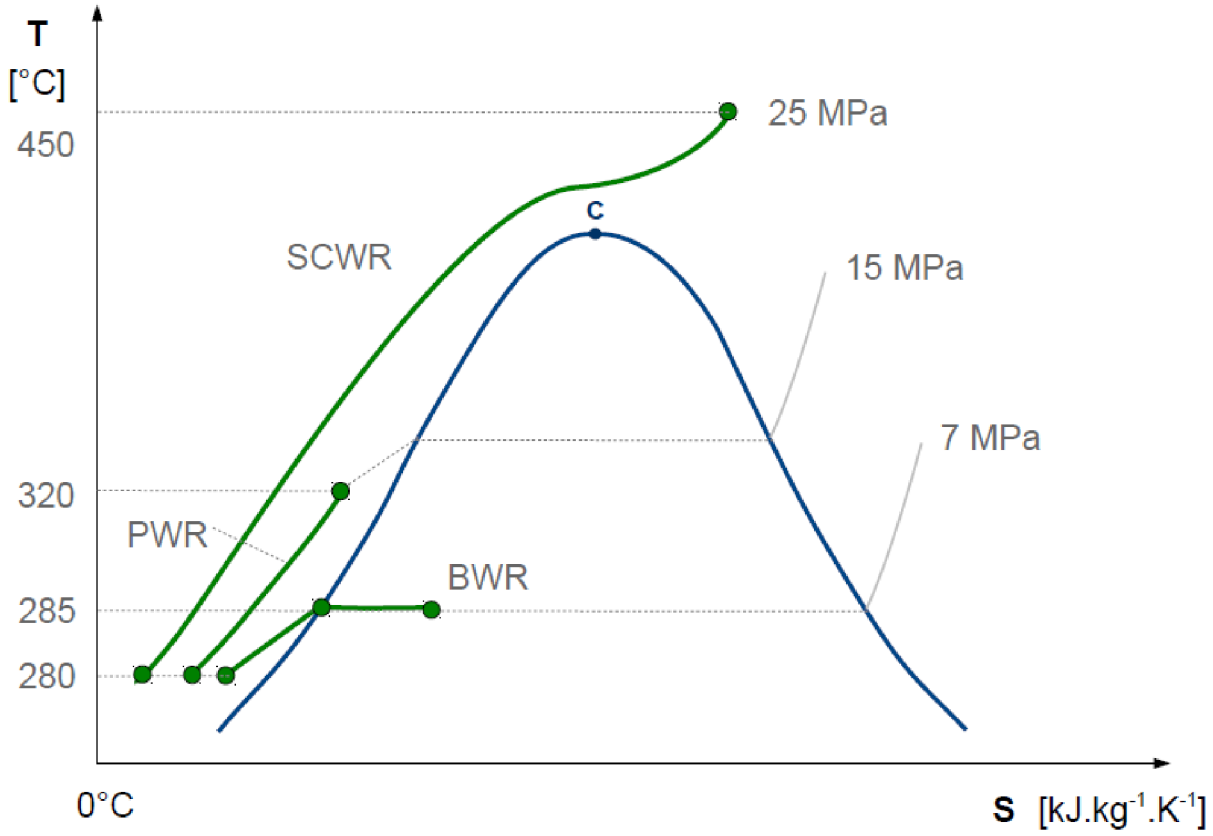

Figure 15: T-S diagram with operating SCWR conditions [17]

The main principle of an energy transformation is a thermal circuit. Due to the validity of the First law of Thermodynamics there is an effort of increasing differences between a heater (the reactor) and a cooler (cooling tower). This is a global tendency at modern heat sources including the nuclear reactors. High-pressure coolant (25 MPa) enters the reactor vessel at the temperature of 280°C. Then it is divided into a downward pit and an upper mixing chamber from where it flows down through special channels – the water rods. These water rods ensure moderation of active zone's neutrons. The coolant is heated up to 510°C in the active zone and formed steam enters a twice reheated cycle. In the Figure 16 the SCWR drawing scheme can be seen [18].

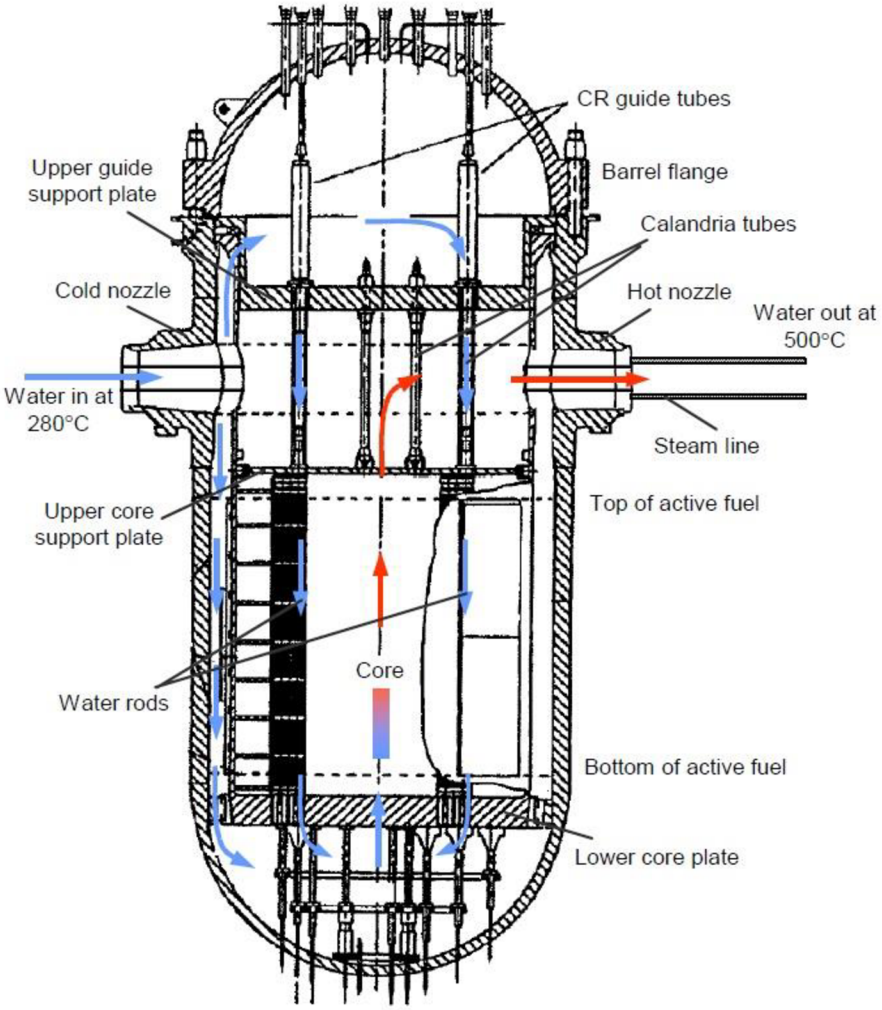

Figure 16: SCWR pressure vessel [19]

2.2.2. SCWL (Supercritical Water Loop)

Most of SCWR's technical problems are connected, rather directly or indirectly, with structural materials. As a main problem stand the thermal-pressure water parameters. The Supercritical water loop serves for researching material corrosion in the environment of intensive radiation and supercritical water radiolysis effects.

SCWL is an active channel where the operating SCWR conditions are simulated. The SCWL scheme is displayed in Figure 17. These conditions are represented by temperature of 600°C and very clear demineralized water at pressure of 25 MPa. The conditions are summed in the Table 6. The active channel is placed to the LWR-15 nuclear reactor after successful inactive assembly and service. The lower part of the channel is immersed to the active zone of the reactor and it is exposed to the neutron flux of $1.5 \cdot 10^{18}$ n/m^{2}s in terms of thermal neutrons and $3 \cdot 10^{18}$ n/m^{2}s in terms of fast neutrons. In Figure 18 there is a photo of SCWL installed in the Czech center for nuclear research in Řež [17].

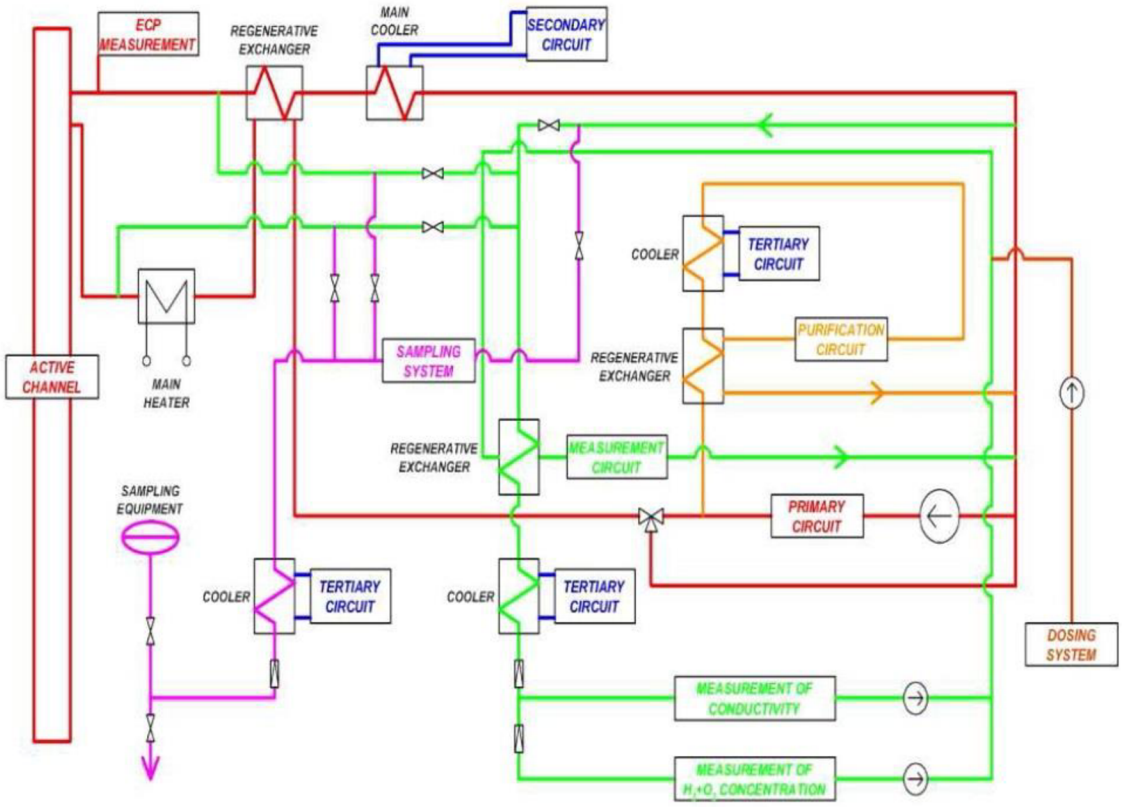

Figure 17: SCWL scheme [17]

There is a global problem with SCWR structural material candidates. Present materials show low values of mechanical properties such are tensile strength or creep rupture properties. However maybe the biggest problem is low corrosion resistance of the materials. Moreover the neutron flux has another inauspicious effect on materials and causes a widening of the dimensions, embrittlement, and radiolysis. After full SCWL assembly and simulation of operating conditions the research process begins. There are 4 main topics that should be tested in this loop [17]:

- Structural materials corrosion in supercritical water with parallel action of the neutron flux
- Water radiolysis and its effect on materials
- Research and testing of a sensor system, especially for measuring of the electro-chemical potential
- Testing a optimization of supercritical cooling water modes

Table 6: SCWL main parameters [17]

Temperature	Loop – 390°C Active channel – 600°C
Pressure	25 MPa (maximum 32 MPa)
Flow	200 – 500 kg/hr
SCWL volume	~42 dm^3

Figure 18: SCWL at ÚJV Řež, Czech Republic [17]

2.3. MSR (Molten Salt Reactor)

2.3.1. Basic information

Salt reactors have its predecessor in MSRE reactor that was tested and developed for bomber engines. Project MSRE was initiated in 1960 at *Oak Ridge National Laboratory*, Tennessee, USA and it should demonstrate the suitability and sustainability of this technology (MSRE is displayed in the Figure 19). Molten Salt Reactors are the only IV generation reactors that use fuel in a melted form. The fuel works also as a coolant and it is in the form of melted salt too. It contains fissionable, generative, or transmuted materials. There is a possibility of draining off the fuel and its changeability. This is a great safety element. With these possibilities there is also an easier fuel preparation which allows making of saline without stir necessity. There is graphite used as a moderator. And the moderator has to be changed every 4-10 years because of radiation damage.

The MSR project is classified among the unclassical systems. The salt reactors could exist in many construction modes. The first type is a salt reactor with an epithermal or thermal neutron spectrum and with a closed cycle. This modification is designed for combustion of plutonium and minority actinides. The second modification is salt reactor with an open fuel cycle for actinide disposal working in a thorium-uranium cycle (Th-U^{233}) with a maximum conversion ratio. The actinide combustion systems should use fuel in form of sodium and zirconium fluorides and the thorium-uranium systems should use fuel in form of lithium and beryllium fluorides. Operating temperatures are expected to be around 565 – 700°C (850°C in case of hydrogen production). Molten salt reactors are planned to operate at atmospheric pressure with the unit power of 1000 MW_e. The secondary circuit should be realized by the Brayton cycle with helium [18].

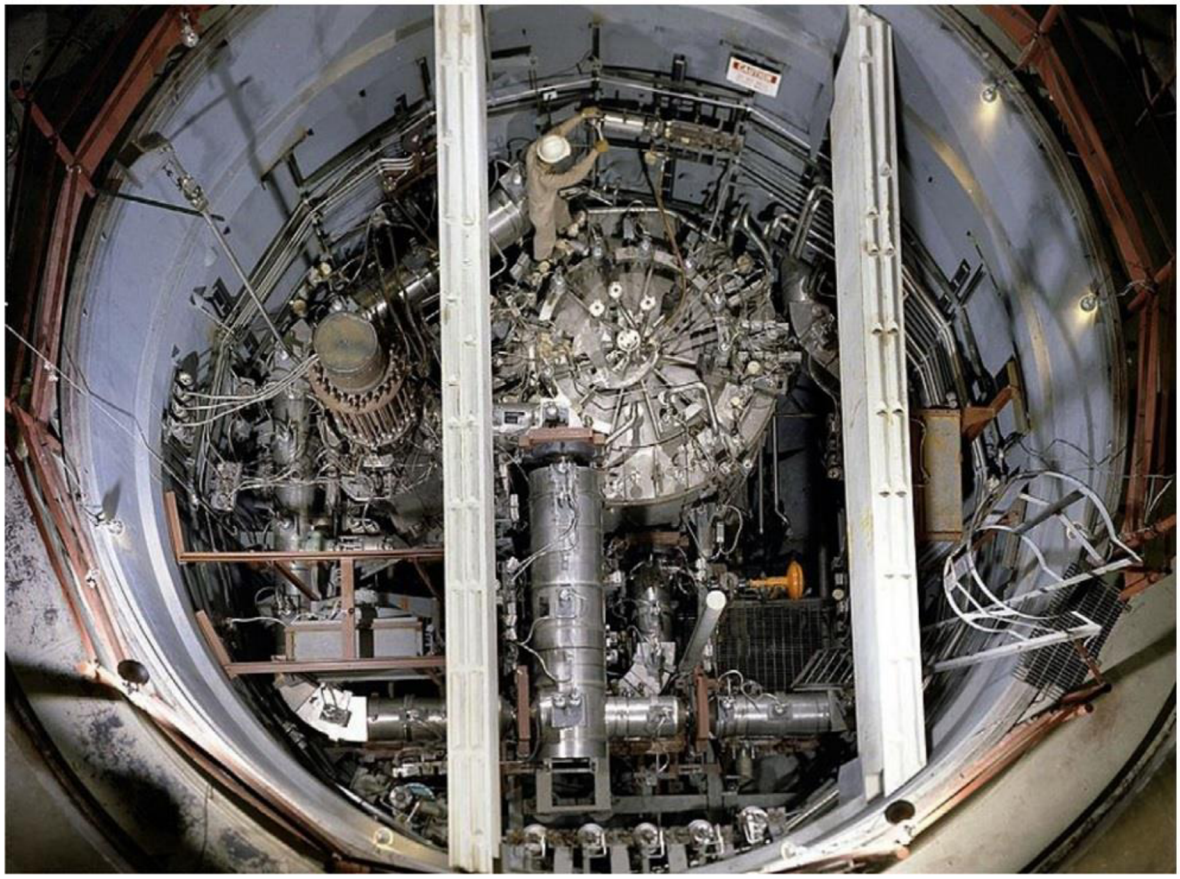

Figure 19: MSRE reactor at Oak Ridge National Laboratory, TN, USA [20]

2.3.2. Material requirements

Graphite is considered as a suitable candidate for core materials. It can be obtained commercially in the near future but it is necessary to improve and discover further the method of its production. Of course, it should be tested properly for salt reactor usage. In a range of operating temperatures there is a huge amount of neutron flux with great energy that causes an appreciable material degradation. Although there are several research results which prove that graphite's radiation resistance could be improved, the development of these methods has not been finished yet. Among considered material belong nickel based alloys as INOR-8, Hastelloy B, Hastelloy N, or Inconel. These materials were used in the past in the MSRE project in 1960s. And they did quite well. INOR-8 is a durable, stable, corrosion resistant alloy with good weldability and formability. Up to 700°C it is compatible with graphite in sodium salts (up to 815°C in non-sodium salts) [18].

Alloy Hastelloy N which was tested in the past is corrosion resistant but it is prone to the embrittlement due to the radiation. Present research results show some progress in newly tested modifications of this alloy. These modifications contain small amount of titanium or hafnium. There should be plenty of tests made to prove and investigate proper materials for MSR usage. For example there is a plan to test Hastelloy N modification long-termly, for couple of years, to investigate its creep rupture properties in fissionable environment. Furthermore there is a process of a material candidate's protection development. This protection is designed as a protective coating in form of frozen oxides. These coatings could be placed on structural material placed in the active zone of the reactor.

2.3.3. Liquid salts

Molten salts seem to be suitable candidates for a nuclear reactor coolant application. It has a great chemical stability at high temperatures (500 – 800°C), a low melting temperature (mostly under 525°C), and a large specific heat and thermal conductivity. The technology of

liquid (molten) salts has been used in plenty of industrial applications such as heat transfer, thermal storage, or heat treatment. The potential of heat transfer capability of molten salts was demonstrated in the MSRE programme at ORNL during the 60s. There were several of molten salts explored and some of them have been investigated in terms of IV generation salt reactor usage. These eutectic salts are called FLiNaK and FLiBe. FLiNaK is an abbreviation for LiF-NaF-KF salt with the composition of 46.5 mol% of LiF, 11.5 mol% of NaF, and 52 mol% of KF. FLiBe stands for LiF-BeF_2 (67 and 33 mol%). Both salts have been recently analyzed in order to support of a fusion reactor, the VHTR transport medium, and the MSR coolant [21].

When speaking about material science these mentioned salts have huge effect on corrosion and oxidation resistance of nearly all the materials. The compatibility of the molten salts with structural steels is related to the potential of oxidation of the structural steel to the appropriate fluorides and chlorides. The molten salt corrosion effects are different in comparison to air or water corrosion. The corrosion in the fluoride fluid salts causes a destruction of passivating oxide layers on the material surface. There are 4 main types of corrosion mechanisms described by the scientific literature: the intrinsic corrosion, the corrosion by oxidizing contaminants, the differential solubility, and the galvanic corrosion. In following subhead there is the FLiNaK corrosion data with action on specific nickel based materials.[21].

2.3.3.1. FLiNaK corrosion data [21]

The data of IV generation material candidates for evaluating corrosion effects of FLiNaK salt is limited. The database for this salt is insufficient and another research and testing are needed. In the Table 7 there are displayed the available corrosion test results.

Table 7: Corrosion rates of various alloys in purified molten LiF-NaF-KF at 850°C [21]

Alloy	Crucible	Test duration [hr]	Corrosion rate [mm/yr]
Incoloy 800H	Incoloy 800H	1000	0.0031
Incoloy 800H	Incoloy 800H	2000	0.0036
Ni-210	Graphite	500	0
Hastelloy X	Graphite	500	0.28
Inconel 617	Graphite	500	0.62
Incoloy 800H	Graphite	500	0.63
Haynes 230	Graphite	500	1.00

The interesting fact can be obtained from these results. The Incoloy 800H has extremely low corrosion rate when the sample is exposed to FLiNaK salt in crucible of same material as the sample is. The value of corrosion rate obtained from measuring with such conditions is 0.003 millimeters per year which is a really low value. In a graphite crucible the corrosion rate of Incoloy is increased to 0.6 mm/yr. It is due to the presence of galvanic couple. Another fact that is worth of mention is that the Ni-210 has no signs of corrosion effects caused by FLiNaK during the 500 hour test.

On the basis of sample mass loss as a measure of corrosion of FLiNaK, tested alloys can be ranked as follows:

Haynes 230 > Inconel 617, Incoloy 800H > Hastelloy X > Ni-210

On the basis of dissolved chromium content as a measure of corrosion, the alloys rank as follows:

Incoloy 800H > Haynes 230 > Hastelloy X > Ni-210

On the basis of grain boundary attack as a measure of alloy degradation, the alloys rank as follows:

Haynes 230 > Incoloy 800H > Hastelloy X > Ni-210

With the usage of available resources the corrosion ranks of materials analyzed in this thesis can be settled. All three rank criterions have the same order:

SS316 > Monel 400 > Hastelloy X > Inconel 718

2.4. Summarization table of generation IV reactors properties

Table 8: Generation IV reactors summary [18]

	VHTR	SCWR	MSR
Power	600 MW_{th}	1700 MW_e	1000 MW_e
Power density ($MW_{th}/m^{3)}$	6-10	100	22
Spectrum	Thermal	Thermal (fast)	Thermal (epithermal)
Pressure	Depends on process	25 MPa	Atm.
Outlet temperature (°C)	1000	510	700 (850)
Efficiency (%)	>50	44	44-50
Fuel	ZrC Coated particles	UO_2	$NaF-ZrF_4$ (BeF_2)
Moderator	Graphite	Water	Graphite
Expected year of technological readiness	2020	2025	2025

3. Analysis of available materials for flange joint

3.1. Wide spectrum of materials

Proper material selection mainly depends on its location in the reactor, on the type of reactor and its environment, on material's characteristics such are corrosion resistance, radiation resistance and so on. There are plenty of proposed material candidates predominantly nickel-based alloys, ceramic composites, monolithic ceramic materials, and ferritic and martensitic steels. As mentioned above many times there are strict demands on the material candidates. Chosen materials are tested in-depth to guarantee its functionality and safety in reactor's environments. Properties such as high-temperature creep, creep rupture resistance, corrosion and oxidation resistance, and tensile strength are especially tested and researched in the ambience of neutron flux and high temperature. Based on the research results further tested materials are ceramics and nickel-based alloys [22].

3.2. Nickel-Based alloys

Nickel-based alloys are the leading candidates for generation IV reactors usage. Some of them have been used in the previous generations. These alloys are characterized by high strengths and good high-temperature corrosion resistance. However there are irreplaceable problems with radiation effects on these alloys. This is why nickel-based alloys are mostly considered as structural materials for heat exchangers and for places out of the active zone. From wide range of material candidates three alloys have been chosen for this thesis: Monel 400, Inconel 718, and Hastelloy X. In the Table 9 their basic characteristics are shown.

Table 9: Chosen nickel-based alloys characteristics [21]

	Monel 400	**Inconel 718**	**Hastelloy X**
Melting range [°C]	1300-1350	1260-1336	1260-1335
Tensile strength of annealed sample (at 1200°C) at room temperature [MPa]	620	1240	767
Thermal expansion at 1000°C [µm/m°C]	18,1	At 760°C 16,1	16,7
Density [g/cm^3]	8,8	8,19	8,22
Declared improved properties	Great corrosion resistance	Great strength, corrosion resistance	High-temperature resistance

Percentage compositions of these alloys are displayed in the Table 10. Each composition has different behavior and effect on material properties. Some of these alloys have been partly modified by adding a precise amount of a certain element. For example by adding of aluminum the oxidation resistance is raised, which causes an increase of corrosion resistance. In further subheads these properties are widened more.

Table 10: Chemical composition of chosen alloys

	Monel 400	Inconel 718	Hastelloy X
Ni	66,5	52,5	47
Cr	-	19	22
Fe	2,5	17	18
Mo	-	3,05	9
Ti	-	0,9	0,15
Al	-	0,6	0,5
Co	-	1	1,5
C	0,3	0,08	0,07
Mn	2	0,35	1
Si	0,5	0,35	1
P	-	0,015	0,04
S	0,024	0,015	0,03
Cu	31	0,3	0,5
Another	-	5,125 Nb+Ta	0,6 W

3.2.1. Monel 400

Monel 400 is a solid nickel-based alloy with good weldability formable only at cold state. It has great strength and toughness at a wide range of temperatures and it is quite resistant in terms of corrosion. Its chemical composition is written in the Table 10 above. Alloy 400 has been recently used in marine and chemical industry in applications such are pump valves, Gimbal or jointed shafts, gas or drinkable water vessels, or heat exchangers.

For usage in IV generation reactors the creep strength is a really important feature. A creep phenomenon appears at materials long-termly loaded by high temperature. The operating environment has a huge effect on creep properties too. If the material is placed in VHTR's helium environment it acts differently than in MSR's salt environment. By that the alloy 400 is suitable for usage in oxidation environments to the temperature of 560°C. For higher temperature it has to operate in reduction environment. In Figure 20 and Figure 21 the creep curves are displayed. Each graph describes different treated sample of Monel 400. The specific treatment is stated below each figure [23].

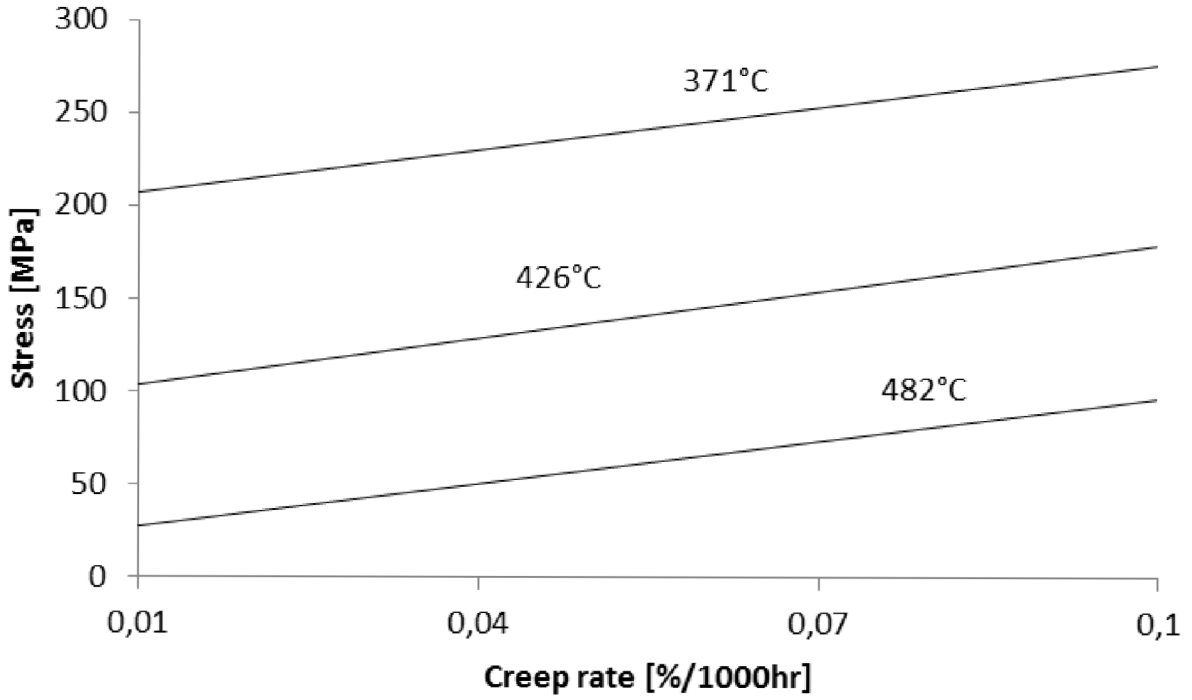

Figure 20: Creep properties of hot-rolled alloy 400 [24]

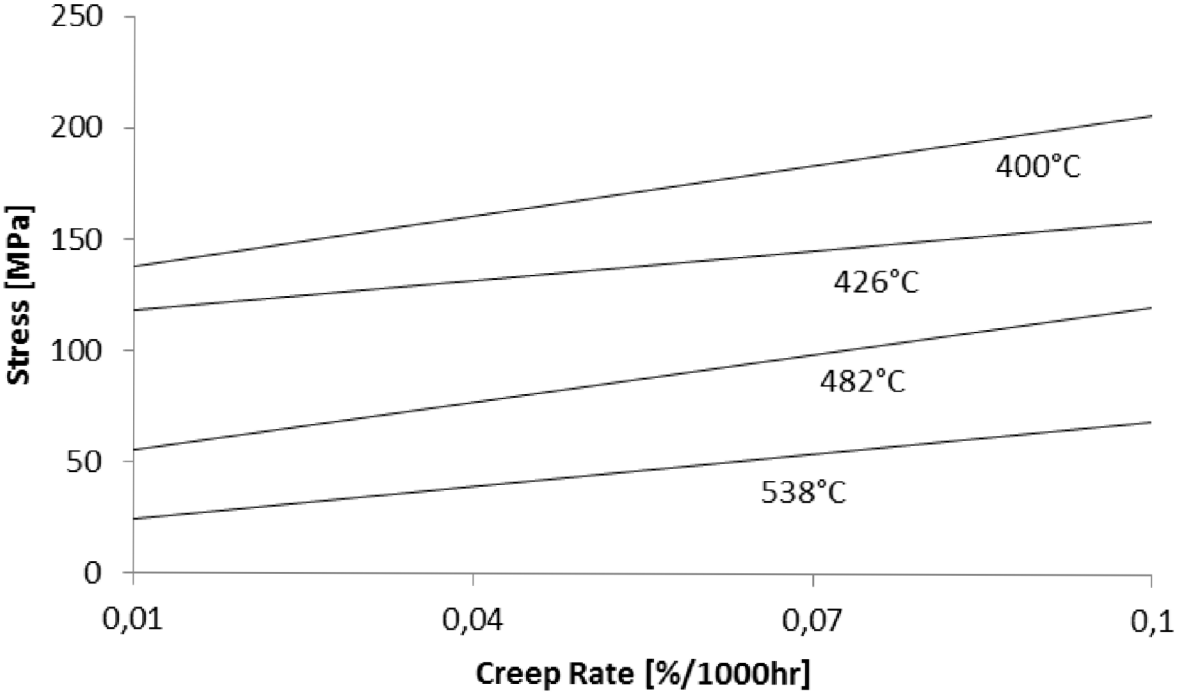

Figure 21: Creep properties of alloy 400 sample cold-drawn annealed at 815°C for 30 minutes [24]

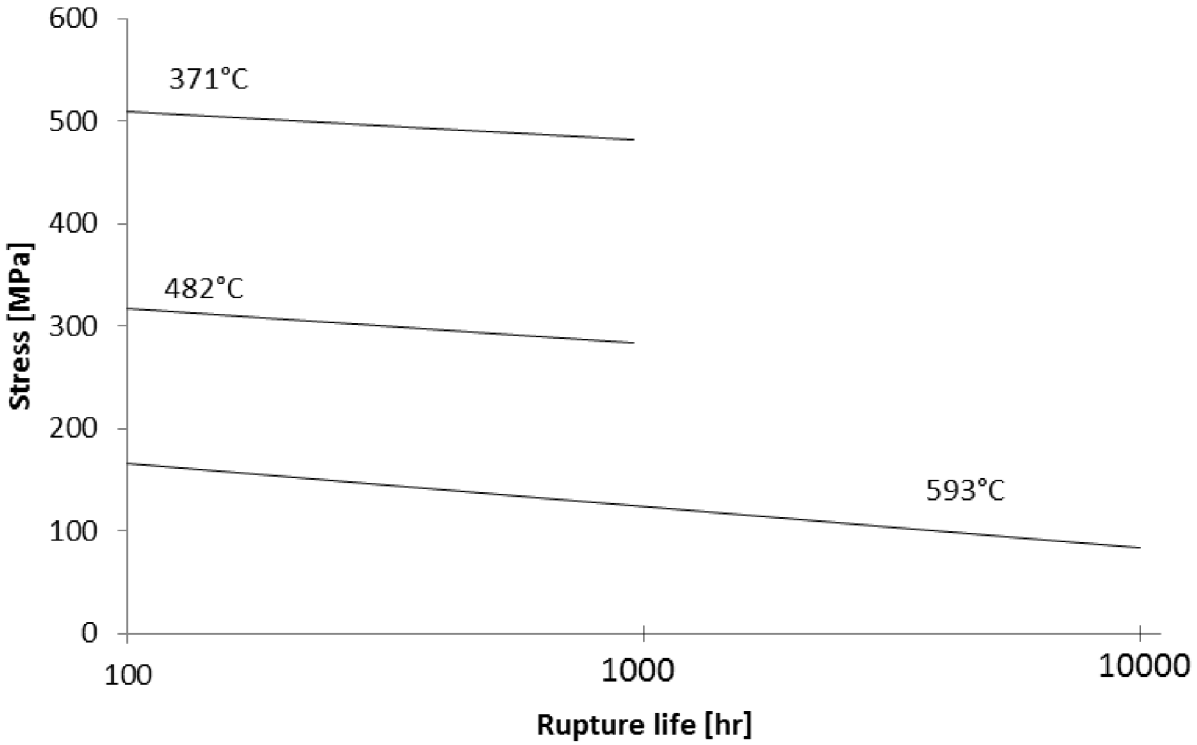

Figure 22: Rupture life of sample cold-drawn annealed at 815°C for 30 minutes [24]

If the material is operated in corrosion ambience it has to resist the environmental effects. Monel 400 shows the corrosion resistance against various reduction environments. It is also more resistant against oxidation environments than the major part of copper alloys. Alloy 400 is abundantly used in water applications. It is resistant against pressure breach and pitting in freshwater and industrial waters. However in flowing seawater the crack initiation and corrosion pitting are recorded.

3.2.2. Inconel 718

Inconel 718 is a high-strength solid chrome-nickel based steel which is corrosion-resistant and can be used in wide temperature range applications (-270°C – 700°C). This age-hardened alloy can be formed into even more complex shapes. Inconel 718 can be welded well with low weld-cracking initiators. Alloy 718 also shows great tensile strength, creep and fatigue resistance, and high-temperature stability. In the present Inconel 718 is used as a structural material of rocket liquid-fueled engines, or as construction parts in aeronautical industry such as engine casings, shafts or other high-stressed components (e.g.: in Airbus a380 Inconel is used for spring shafts, or wheel and braking system parts). It is also used as structural material of gas turbine engines, or cryogenic chambers [25, 26, 27].

Because of possible high temperature operation the high-temperature creep, corrosion resistance, and mechanical properties are mainly tested. Creep is permanent high-temperature stress deformation. For nuclear reactor usage the tests have to be made also during radiation process (e.g.: neutron flux). Due to the strong radiation reactor's field has strong effects on material properties. In following figures the stress-life dependencies within different temperatures are displayed (Figure 23), dependency of pressure on creep rates (Figure 24), and dependency of shear strain values on irradiation intensity at 300°C and different pressures (Figure 25).

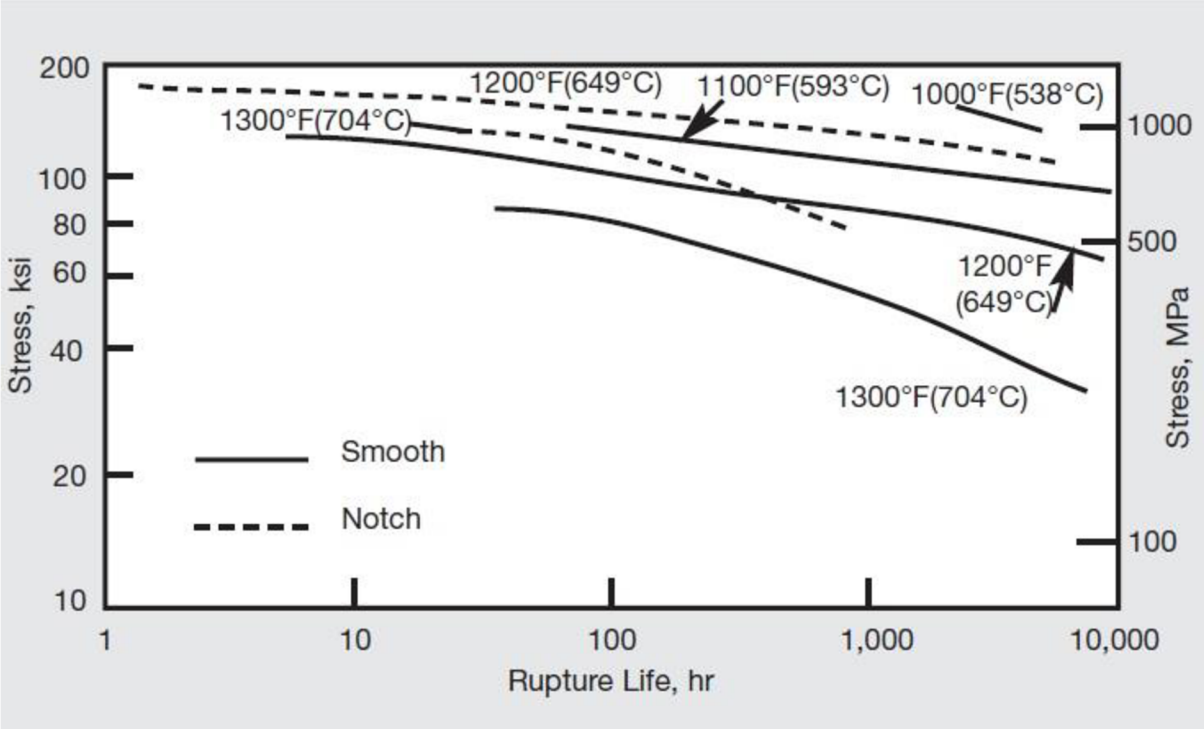

Figure 23: Rupture Life curves [25]

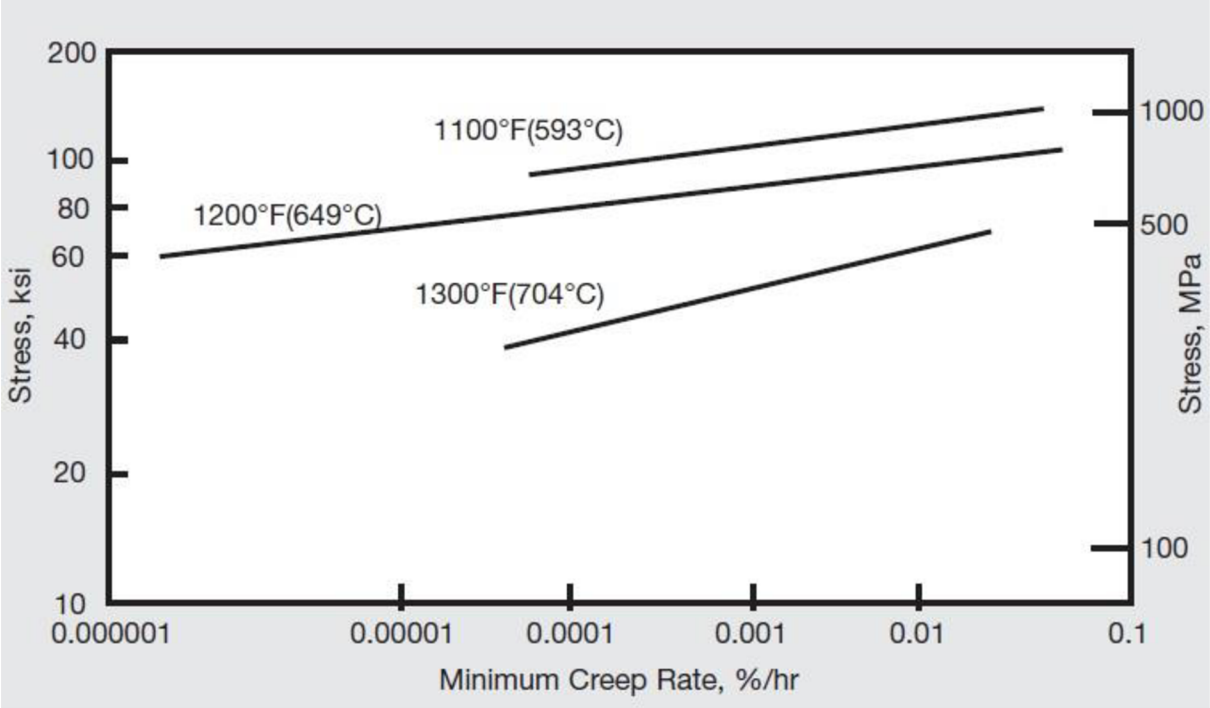

Figure 24: Minimum Creep Rate curves [25]

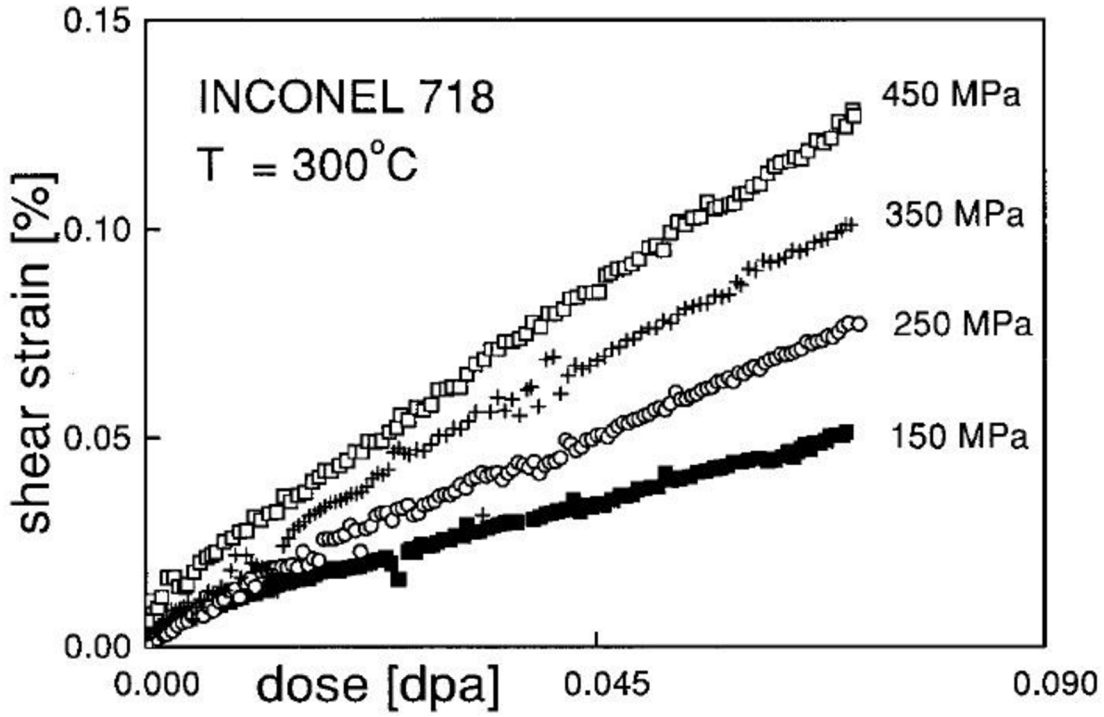

Figure 25: Shear strain on irradiation effects dependency [28]

Mechanical properties and high temperature deformation effects belong among leading issues that show the suitability of each material for generation IV needs. Extraordinary needs have to be met in VHTR because of the present high temperatures. The amount of alloying elements has essential effect on material behavior. Mechanical strength of superalloys can be increased by adding elements of Al, Ti, Nb, Co, Cu, and W. These elements contribute to the elevation of tensile and yield strength. In the Figure 26 there are yield and tensile strength curves with the elongation effect of a test sample (Figure 27).

The multiple environment resistance of alloy 718 is caused by nickel, chrome, and molybdenum alloying elements. The existence of nickel protects the material from corrosion, oxidation, and carburation in many environments both alkaline and acidic. The greater amount of chrome obstructs a degradation of the material caused by sulfide compounds and oxidation media influence. The amount of molybdenum contributes to pitting protection. Nickel and chrome crystallize as γ phase (face centered cubic) which makes up a basic matrix of alloy 718. To form hardening precipitates antimony is added. Antimony creates metastable compounds Ni_3Nb which make up γ`` phase in form of centered tetragonal crystal. Titanium and aluminum precipitate as intermetallic phase γ` as Ni_3Ti and Ni_3Al compounds with cubical crystal. All of these phases can precipitate at grain boundaries [29].

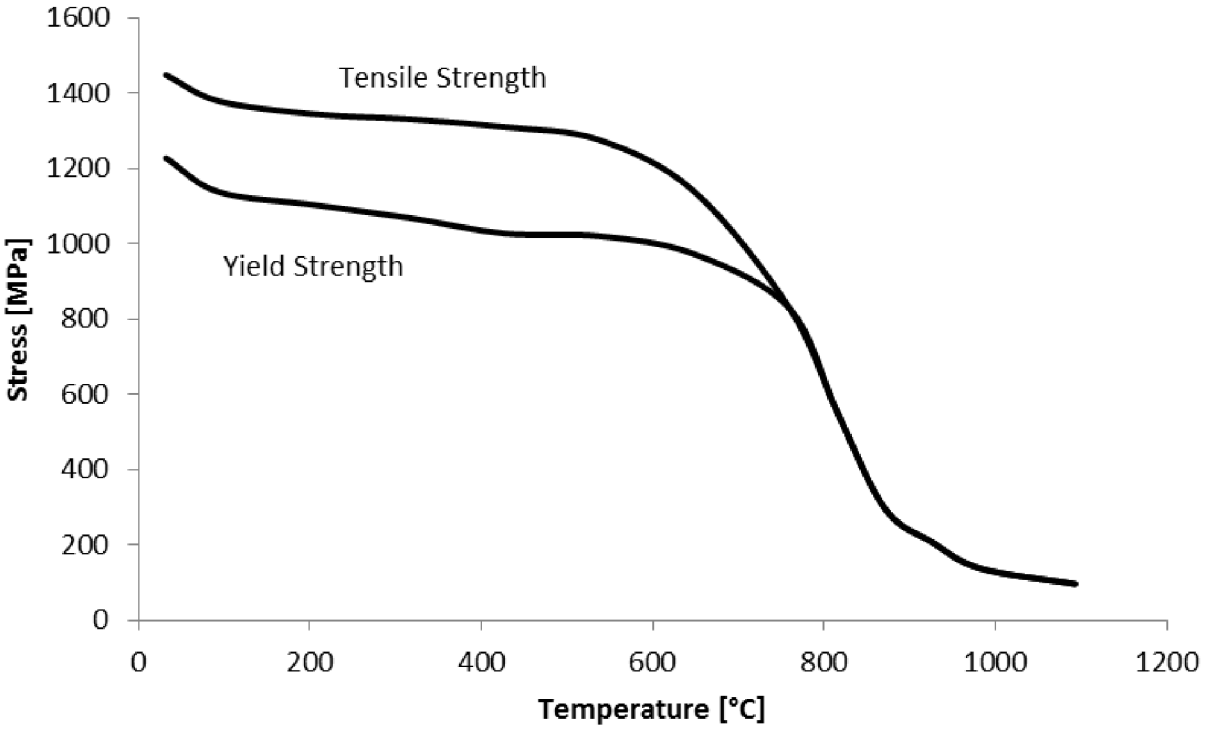

Figure 26: Mechanical properties at different temperature values [25]

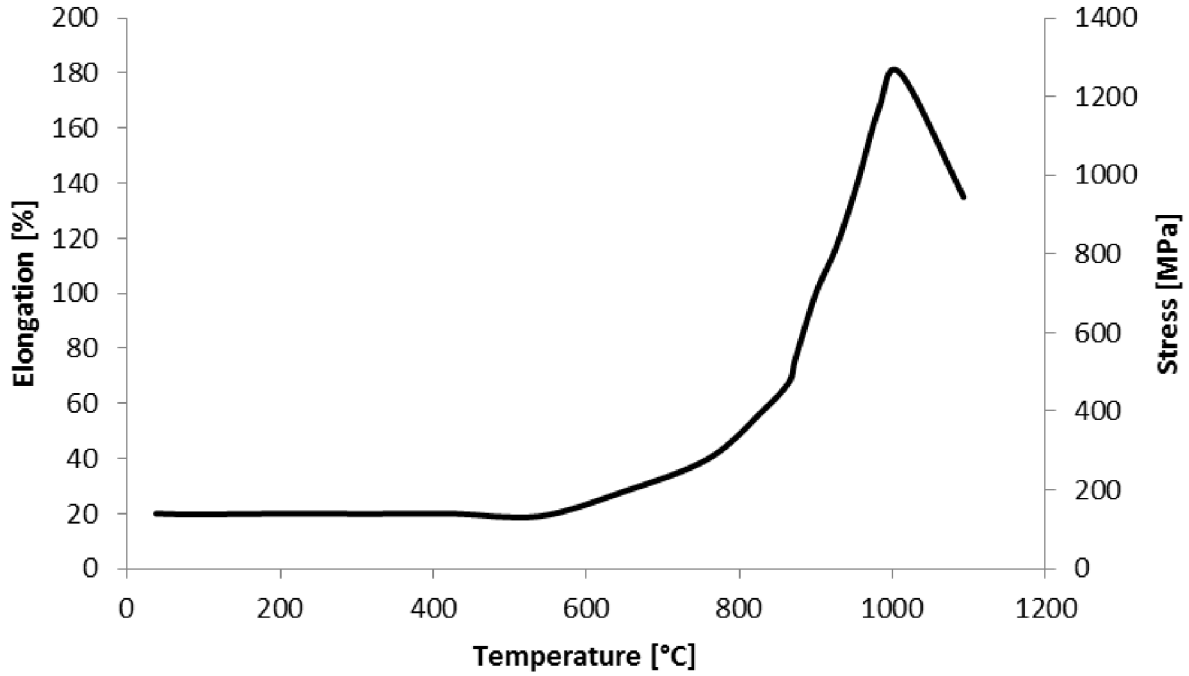

Figure 27: Stress-elongation curve depended on temperature [25]

In the pictures the typical high temperature material behavior can be seen. As it results from the figures the yield strength curve merges with the tensile strength curve at the temperature around 760°C. And at the temperature around 1100°C the Inconel 718 has the tensile strength still above the value of 100 MPa. But the elongation approaches to value of 180%. In the following Figure 28 the stress-strain curves are displayed each with different strain rate ratio.

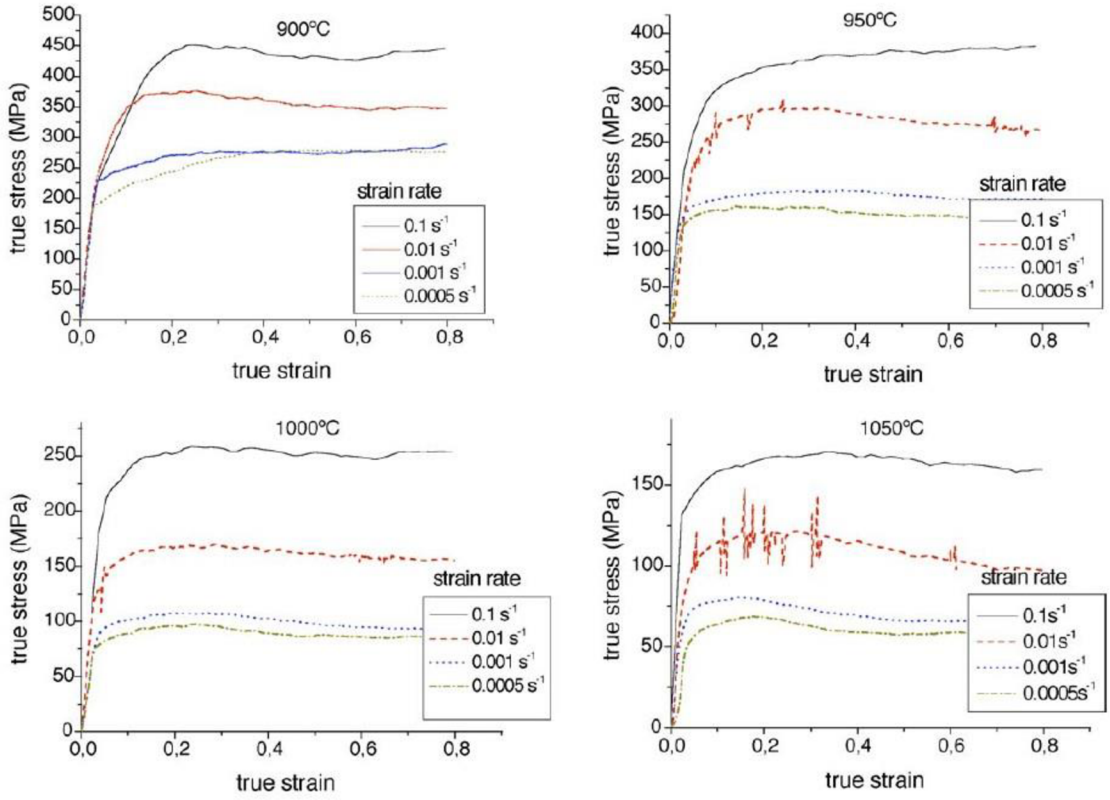

Figure 28: Flow curves for Inconel 718 [29]

Other properties that describe tested materials are density, heat conductivity, and heat capacity. As well as the other properties these three issues are temperature dependent too. The problem is that mathematical function of density dependence has to be determined statistically. There are many experimental data from which the mathematical equations were determined. Some of the experimental values are in great agreement so there is no problem with the equations compilation. But if there are some negligible difference compromises that have to be made [15].

The density of Inconel 718 is described with 2 equations (for solid and liquid phase). In the Figure 29 the density dependence is displayed.

$$\rho_s \cong 8190 - 0.392(t - 25°C) \quad (1)$$

$$\rho_l = 7400 - 0.88(t - 1336°C) \quad (2)$$

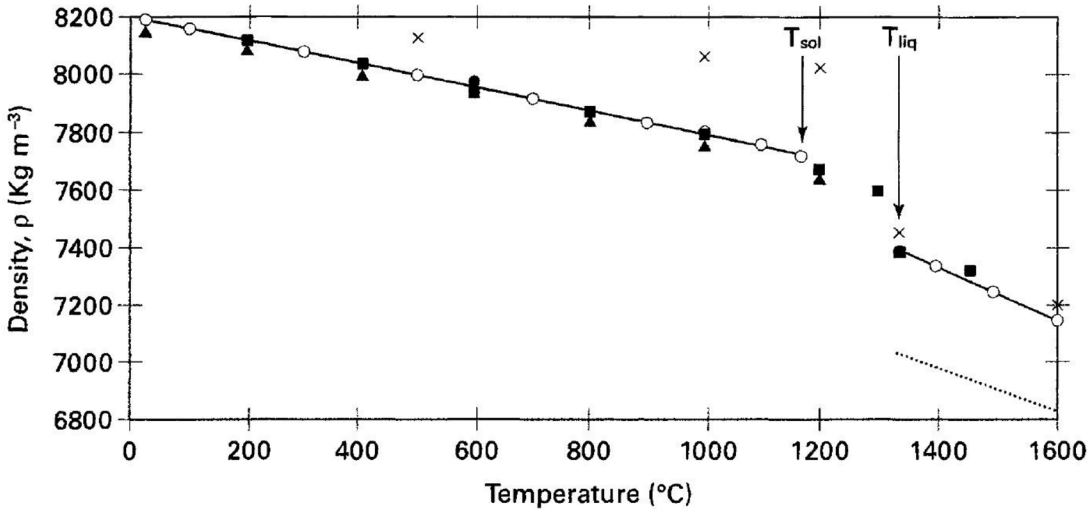

Figure 29: Density of Inconel 718 as a function of temperature [15]

Beneath symbol ▲ are values measured by Overfelt [30], symbol ■ are values from Henderson [31]. The line displays recommended values of density.

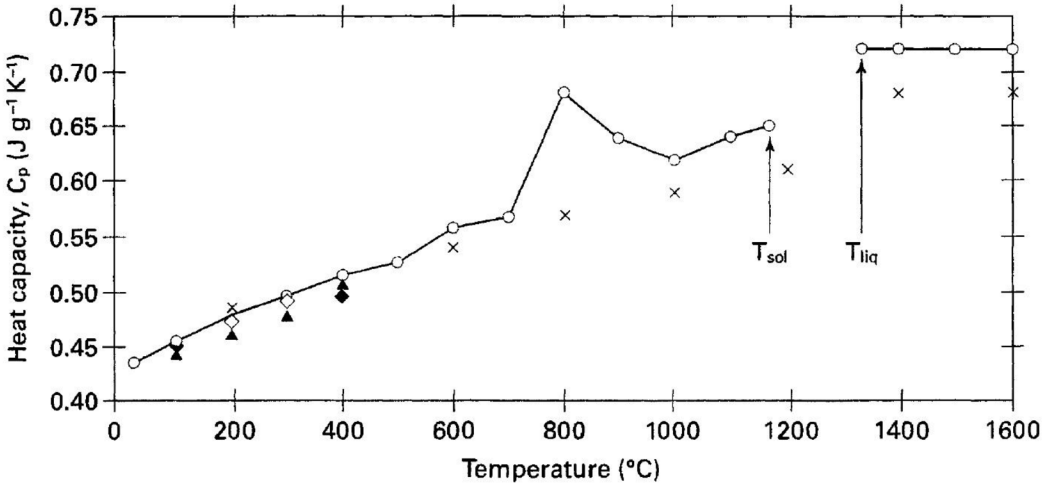

Figure 30: Heat capacity of Inconel 718 as a function of temperature [15]

The recommended values of Inconel's heat capacity were measured and formed by Richardson [32].

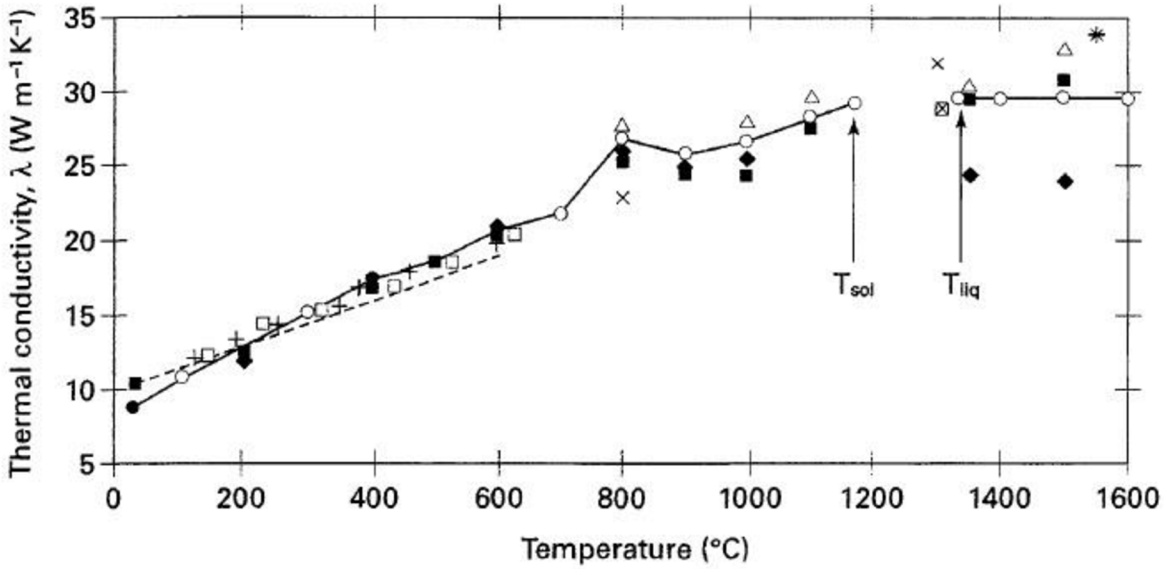

Figure 31: Thermal conductivity of Inconel 718 as a function of temperature [15]

3.2.3. Hastelloy X

Hastelloy X alloy is another one from the high-strength and great corrosion resistant alloy itinerary. It is a commonly used material in furnace applications and in aeronautical industry for turbine-engine outlets production (or other components). This alloys shows good high-temperature stability. Similarly to Inconel 718 has Hastelloy X good formability and it is suitable for welding. Hastelloy X has already been chosen as a structural material of transfer pipes and IHX hot header for Japanese VHTR. A modification of alloy X has been made to increase the helium coolant compatibility of the material. This modification is called Hastelloy XR. The difference between alloy X and XR is written in the Table 11 below [22, 33].

Table 11: Hastelloy X and XR chemical composition [34]

	Hastelloy X	Hastelloy XR
C	0,07	0,007
Mn	0,61	0,83
Si	0,39	0,32
P	0,012	<0,005
S	<0,001	0,006
Cr	21,26	21,84
Co	1,71	0,19
Mo	8,89	9,06
W	0,57	0,53
Fe	18,98	18,26
B	<0,001	<0,001
Ni	Balanced	Balanced
Al	-	<0,05
Ti	-	<0,05

As mentioned above the Hastelloy X has good high-temperature properties so that it is considered to use in VHTR structural components. The high-temperature creep is the main tested feature. Alloys like Hastelloy (X, XR) and Inconel (617, 718, or 800) show minimal

high-temperature deformation. As it can be deduced from figure 32, the material reinforcement occurs by the influence of plastic deformation to the temperature of 750°C. After a maximum stress level at 950°C is reached there are no reinforcement effects on samples [22].

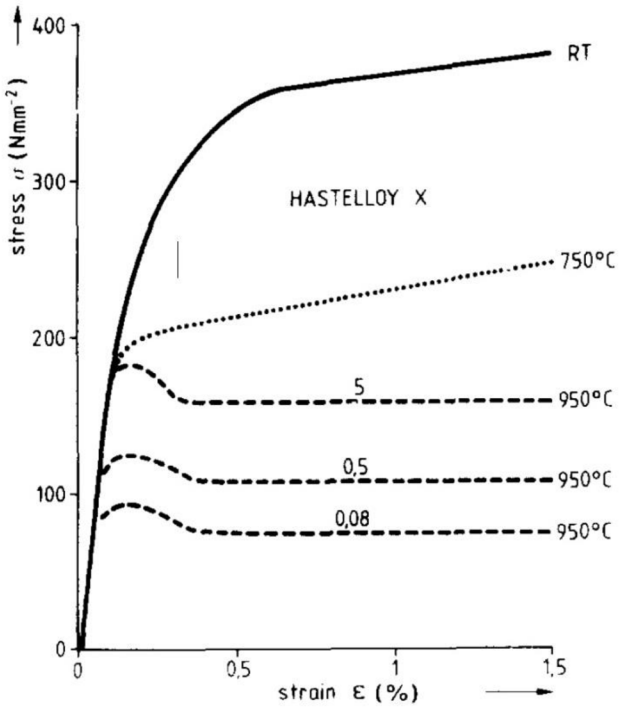

Figure 32: Hastelloy X, stress - strain curves at high temperatures [35]

The modified XR alloys is intended to use in VHTR and it shows in simulated helium environment creep test similar strain values as the Inconel 718 but less service life. Results of this test are shown in Figure 33. There are 4 curves each one is for different mode of neutron flux.

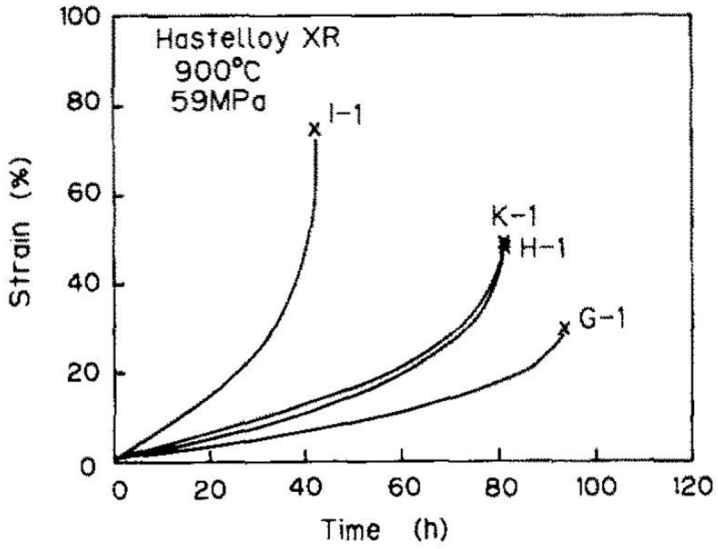

Figure 33: Helium environment creep curves [36]

Creep properties can be also evaluated from other experimental measuring. The material sample is located in a helium filled chamber and exposed to the temperature of 1000°C. This sample is stressed by constant pressure at first and second creep stages. Durations to rupture

are recorded into tables for comparison. Tables 12, 13, and 14 show results of experimental test at different temperatures where in table 11 the first stage of creep is recorded, in Table 12 the second stage, and in the Table 13 the time to rupture and total elongation values are summed.

Table 12: Hastelloy XR, creep rupture test - First stage [37]

1^{st} stage				
Test number	**Temperature [°C]**	**σ_1 [MPa]**	**Δt_1 [hr]**	**$\Delta \varepsilon_1$ [%]**
1	850	31.4	1961	2.0
2	850	34.7	1250	2.1
3	850	46.5	504	5.4
4	900	19.8	4250	3.9
5	900	28.4	792	4.4
6	900	33.3	533	7.9
7	900	43.2	151	11.0
8	950	14.7	822	2.0
9	950	14.7	2040	3.0
10	950	19.6	768	7.0
11	950	19.6	1008	9.3
12	1000	8.2	3312	5.3
13	1000	9.8	840	4.4
14	1000	14.4	560	5.4

Table 13: Hastelloy XR, creep rupture test - Second stage [37]

2^{nd} stage				
Test number	**Temperature [°C]**	**σ_2 [MPa]**	**Δt_2 [hr]**	**$\Delta \varepsilon_2$ [%]**
1	850	46.5	694.3	30.3
2	850	46.5	955.2	31.2
3	850	34.7	2894.3	10.9
4	900	28.4	486.6	13.1
5	900	19.8	4662.0	8.1
6	900	43.2	105.2	27.9
7	900	33.3	489.1	14.3
8	950	19.6	1017.7	19.
9	950	22.8	327.5	18.3
10	950	14.7	1202.5	5.7
11	950	15.2	208.4	3.0
12	1000	14.4	235.5	15.5
13	1000	14.4	776.4	16.4
14	1000	8.2	2972.3	8.6

Table 14: Hastelloy XR, summary of creep-rupture test results [37]

Test number	Time to rupture $\Delta t_1 + \Delta t_2$ [hr]	Rupture elongation $\Delta \varepsilon_1 + \Delta \varepsilon_2$ [%]
1	2655.3	32.3
2	2205.2	33.3
3	3398.3	16.3
4	4736.6	17.0
5	5454.0	12.5
6	638.2	35.8
7	640.1	25.3
8	1839.7	21.8
9	2367.5	21.3
10	1970.5	12.7
11	1216.4	12.3
12	3547.5	20.8
13	1616.4	17.8
14	3532.3	14.0

Mechanical properties of Hastelloy X are also tested at high temperatures. In the Table 15 the values of tensile strength, yield strength and elongation are showed. The decrease of tensile and yield strength is obvious at temperatures between 900 and 1100°C.

Table 15: Hastelloy X, mechanical properties at high temperature [33]

Form	Condition	Test temperature [°C]	Ultimate Tensile Strength [MPa]	Yield strength at 0.2% offset [MPa]	Elongation in 50.8mm [%]
Sheet (1.1-1.5mm) thick	**Bright annealed at 1177°C, hydrogen cooled**	Room	767	379	44
		538	614	245	49
		649	581	244	54
		760	463	237	53
		871	310	194	59
		982	177	91	66
		1093	97	43	60

Due to VHTR usage the corrosion resistance is one of the most important features. Corrosion caused by the helium impurities like hydrogen, water, carbon dioxide, and methane have negative influence on tensile and yield strength and creep resistance. A level of corrosion is proportional to the amount of impurities in the helium.

Similarly to Inconel 718 Hastelloy X's properties such as density, heat capacity, and thermal conductivity are temperature dependent. The equation 3 describes density dependence of solid phase of Hastelloy X and the equation 4 dependence of liquid phase. The complete dependence is displayed in the Figure 34.

$$\rho_s \cong 8240 - 0.381(t - 25°C) \quad (3)$$

$$\rho_l \cong 7240 - 0.83(t - 1355°C) \quad (4)$$

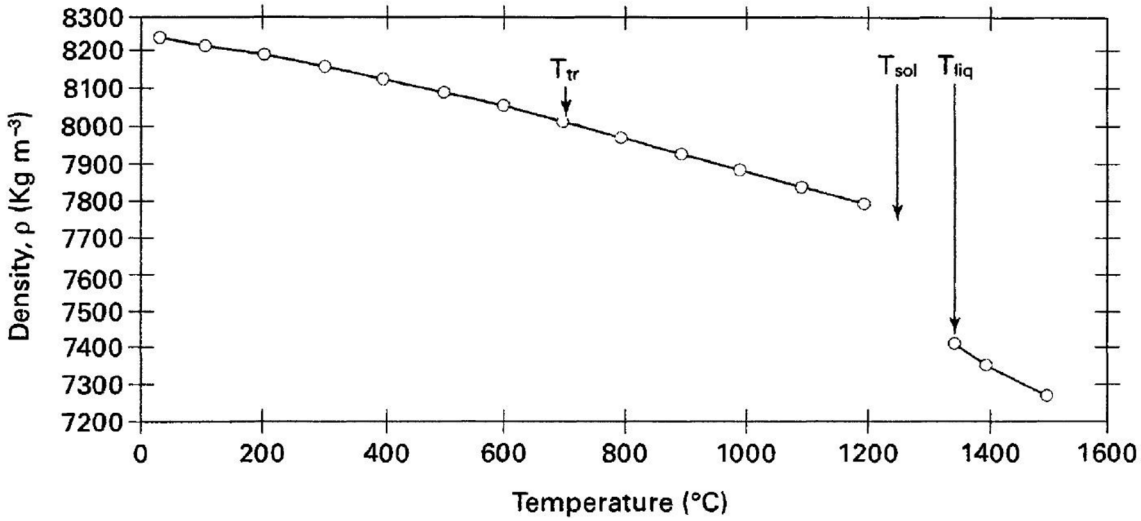

Figure 34: Density of Hastelloy X as a function of temperature [15]

Heat capacity values are displayed in the Figure 35. Measured values are in good agreement up to 600°C. At this temperature there is an increase of C_p and transition alloy behavior occurs. The values for liquid phase have to be estimated because no values have been reported [15].

Values with ▲ and ○ symbols are measured by Taylor [15] and values with --- symbols are reported by Maglic [38]. Values with X symbol are estimated values.

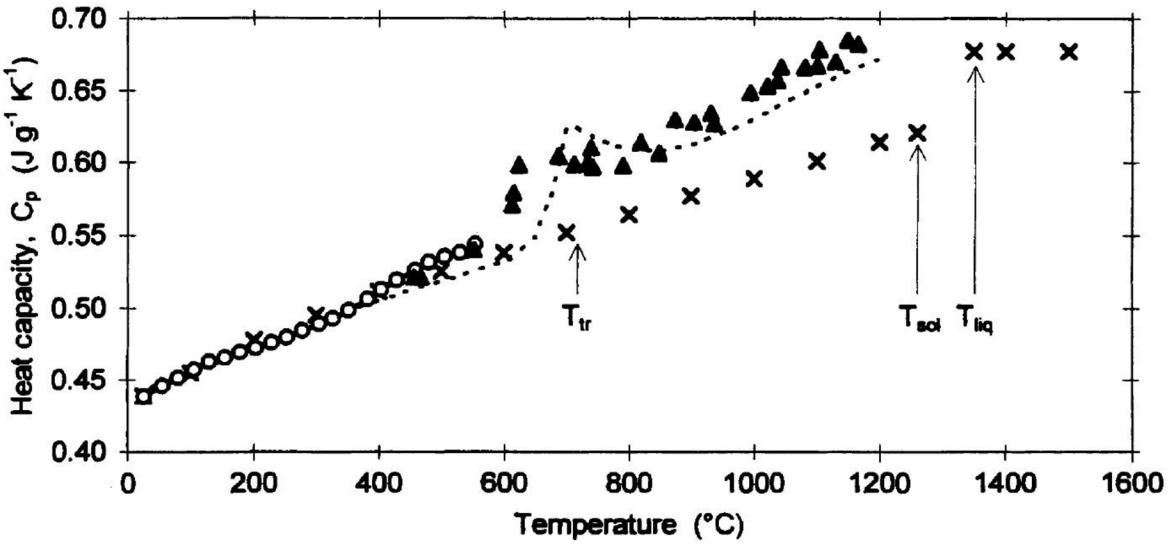

Figure 35: Heat capacity as a function of measured values [15]

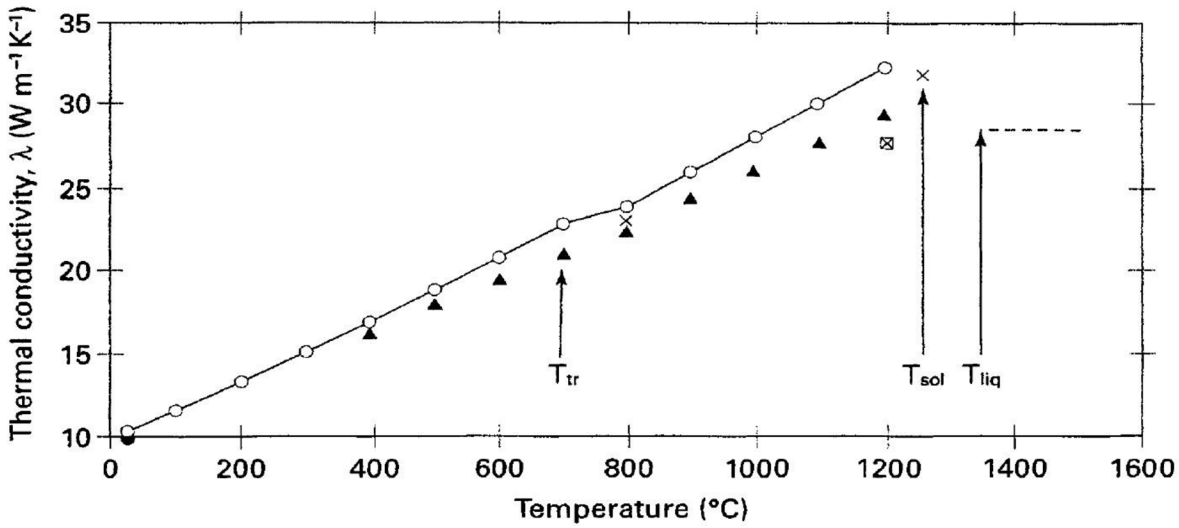

Figure 36: Thermal conductivity of Hastelloy X as a function of temperature [15]

○ values are reported by Maglic [38] and ▲ values by Neumann [15].

3.3. Assessment of suitability of chosen nickel-based alloys for VHTR heat exchanger flange joint

VHTR heat exchanger (or IHX) is a device which transfers the heat from the primary circuit to the secondary one. It means that it transfers primary heat with temperature of 850 – 1000°C to the secondary with temperature around 800 – 900°C. The heat transfer is mediated by helium coolant. IHX also keeps the secondary circuit free from the radioactive contamination. The stresses in the exchanger are quite low (around few bars during normal service and 6-7 MPa during off-normal events).

From available materials that are analyzed in this thesis the Inconel 718 seems suitable for this application. It is great-strength material at high temperatures. As it can be seen in subhead 3.2.2, the tensile strength value is held above 100 MPa within temperatures above 1000°C. In terms of creep resistance the Inconel 718 shows great creep-rupture properties. But when speaking about IHX where the stresses are not that high the corrosion resistance and stability under neutron flux are the main challenges for this application. Protective weld layers can be used to protect the material surface from neutron flux as mentioned in subhead 2.1.5.1. The corrosion resistance is performed by alloying elements in material but helium is really strong reagent so it causes reduction of mechanical properties as the creep rupture life. Helium reacts with chromium alloying element and causes corrosive oxidation and carburization. This corrosion effect can be lowered by greater amount of manganese in chemical composition. Due to this fact the Hastelloy X seems to fit, and the Hastelloy XR even better, to IHX application in terms of corrosion resistance. That is why it has been chosen for Japanese VHTR system. Material properties of Inconel 718 and Hastelloy X are quite similar. Inconel can sustain greater stresses in high-temperature environment but Hastelloy X is more resistant towards helium effects. For IHX application the corrosion resistance and the radiation stability demands are much more emphasized than the mechanical one. It is because operating conditions mentioned above. Inconel 718 definitely can be used in some VHTR applications but for IHX flange joint Hastelloy X (and Hastelloy XR) seems to be more suitable.

Monel 400 is not suitable for IHX because of its low integrity at temperatures higher than 600°C. But the further research of more material candidates has to be continued. Mainly in area of helium corrosion and neutron flux effects.

4. Experimental proposal of substitution by new materials

4.1. Description of the experiment

The aim of this experiment is to show suitability of Inconel 718 for the replacement of the stainless steel 316 in flange joint seal application and its connection suitability by electron beam welding. The stainless steel is commonly used alloy in high temperature applications like the heat exchangers. However this steel does not meet with the requirements for VHTR intermediate heat exchanger or other part of IV generation reactors, it has to be replaced by a new material. In this chapter the electron beam welding effect on both materials is discussed in order to valorize this substation method, and then the scheme of the experimental device is displayed. In the Figure 37 there is a photo of the experimental stainless steel flange with the seal and in the Figure 38 there is the seal separately. All parts are made of stainless steel 316.

Figure 37: Detailed stainless steel flange

The experiment itself should test particular combinations of the flange joint constructional types with their sealing materials. These parts will be exposed to the temperatures up to 1000°C and the degradation dependency on outer atmosphere will be recorded and assessed. The outer atmosphere will be variable and it will be changed from inertial to strongly oxidizing. The most suitable constructional part from this part of the experiment will be used in the second stage. The experimental second stage takes in account the inner overpressure and it is widened in the subhead 4.4.

Figure 38: Welded seal

4.2. Electron Beam Welding

The electron beam welding is a process of an energy transmission to a certain point and the materials are connected with each other. The transmission is mediated by the electron beam. The working place has to be evacuated (the vacuum is needed) to apply this technology. This condition partly extends costs of welding but it is also an advantage because there is no contamination of the welded joint by undesirable gases such as nitrogen, oxygen, or hydrogen. The electrons cannot penetrate to the whole width of the material. However there is the deep-size effect caused by electron beam welding method so that the materials of the width of 300 mm in terms of stainless steel and 200 mm in terms of copper can be welded at one beam pass. The material is heated up to its evaporation temperature and the nascent steam displaces the melt to sides. After this action the capillary is created (often named as keyhole), which allows the beam to penetrate deeper. The electron beam heat affected area is much smaller than the arc welding one. Because of the tight affected zone the weld properties such are the deformation, the volumetric shrinkage, and internal stress initiators are low [39].

4.2.1. Welding Inconel 718 – Problems and microstructure

The nickel based alloys are generally not that weldable as the steels. There are plenty of problems that can occur. The main problems are with a creation of weld-cracks due to the high welding temperature or due to the crack presence in the heat affected area. Every single nickel alloys has a different welding properties.

There are several problems with welding of Inconel 718. First of all there is problem with the lack of integrity of the welds. Bad penetration is caused by poor fluidity of the molten metal. This phenomenon can be removed by a correct choice of the protective gas, the root gap width, and the correct weld preparation (in terms of weld purity and proper electron beam properties). Microfissuring is a creation of micro cracks in heat affected area and it is also another problem which can occur when welding alloy 718. The microfissuring can be avoided by usage of a heat treated material below 1050°C and an energetic-wealth beam. Finally the leak of ductility can be met after the welding process. This deficit is removable with high-temperature annealing at the temperature of 1060°C [40].

The weld quality and other properties of welds can be obtained from metallographic microstructure studies. The proper material penetration can be investigated or the differences of microstructure between heat affected zone (HAZ) and fusion zone (FZ) can be seen. In the Figure 39 the cross-sectional micrographic view captured by SEM is displayed. The HAZ is an Inconel 718 weld captured by SEM is developed by precipitation of δ and σ phases in grain boundaries of base material and fusion zone [41].

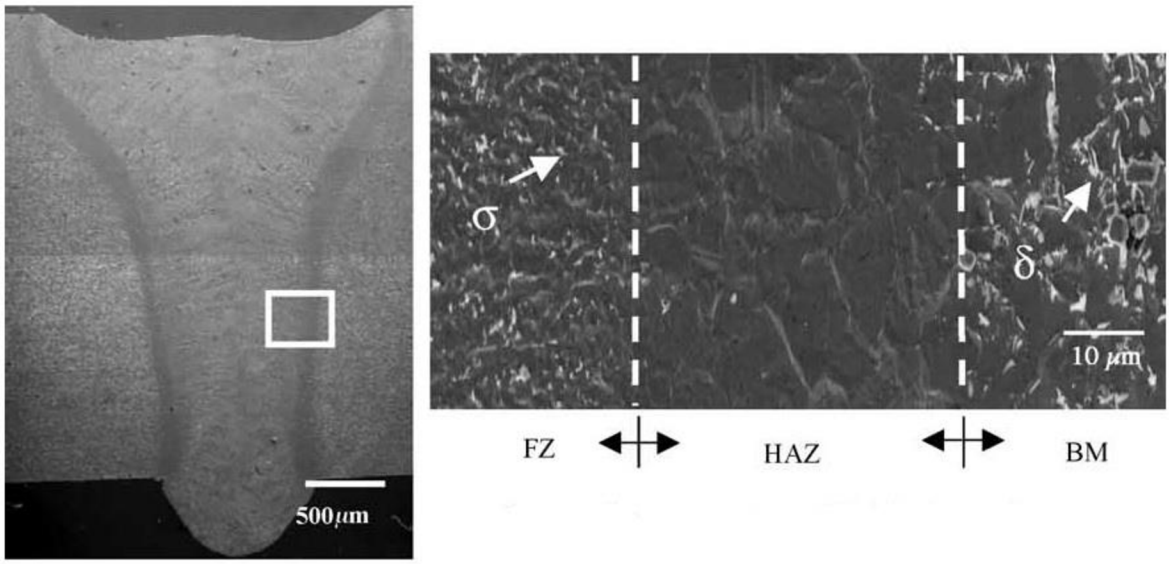

Figure 39: Cross-sectional view of solution-pretreated weld captured by SEM [41]

4.3. Electron Beam Welding of SS 316

At the first stage of experiment the test sample from stainless steel is welded with the EBW process. The metallographic cross-section is made to investigate the weld's quality and properties. There were made two types of welds. One type is welded with the beam of diameter of 0.3mm and the second one with 0.5mm diameter. Both sections are displayed lower as Figure 40 and Figure 41.

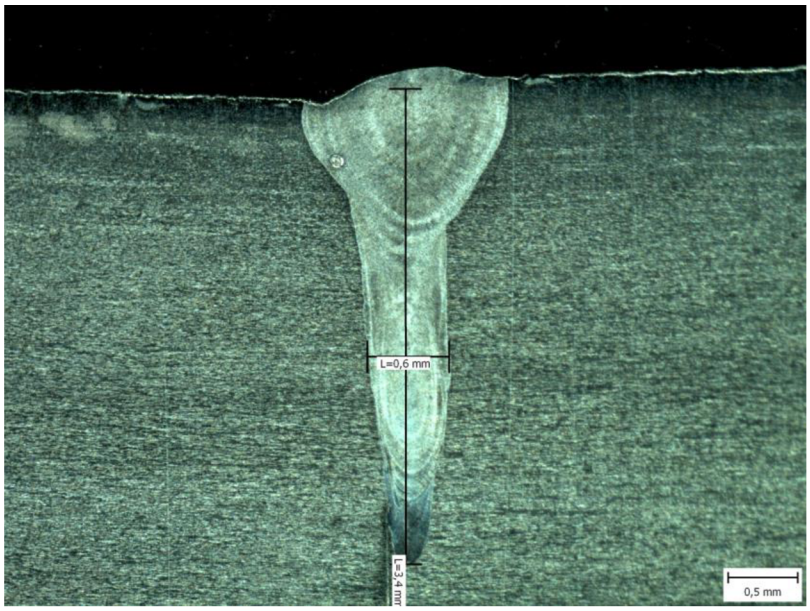

Figure 40: EBW of SS316 with 0.3mm beam

Welding with the beam diameter of 0.3mm is not much suitable for flange joint because the beam is really thin and there is a danger that the joint can be missed by the beam. Also the weld peak is a little bit askew. And the weld roots are not straight at the weld middle. This can be avoided at the final product but still there is the danger of a small deviation of the shape of weld curve. These issues can be removed by usage of larger beam as is displayed in the Figure 41.

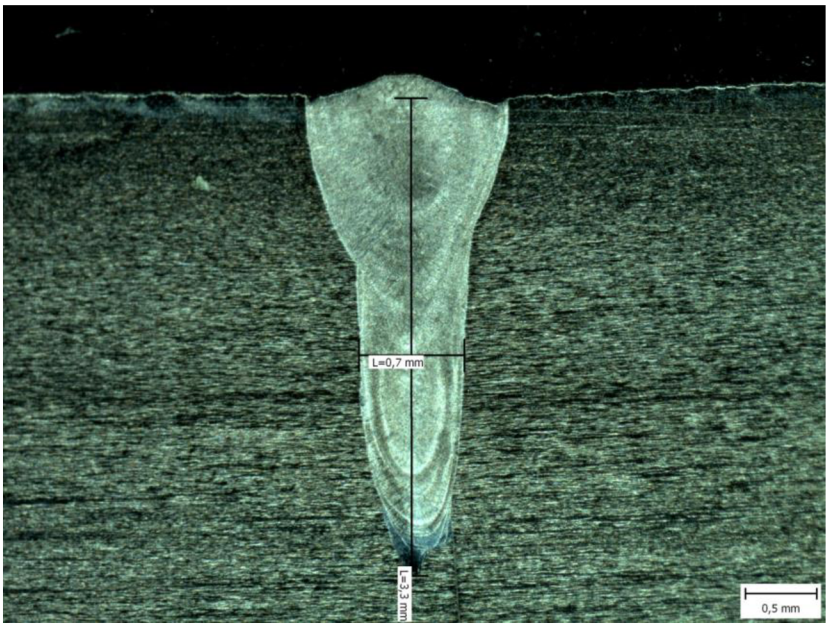

Figure 41: EBW of SS316 with 0.5mm beam

This weld seems to be better. All weld roots come from the middle and the peak is quite narrow. Also the penetration seems to be superior to previous. The weld could be made with

larger diameter of the electron beam but it would result to the greater amount of produced heat and to the bigger deformations.

4.4. Scheme of the experiment

After an identification of the suitable flange construction modes from the first part (which is detailed in the subhead 4.1) the experiment will continue. In this part an inner pressure is added beside the temperature load. The inner pressure will be brought into the flange by an inlet pipeline. This pipeline will be headed through a wall of a furnace by a temperature-resistant channel. Complete experimental equipment, which is display in the Figure 42 in form of a scheme, will consist of the flange joint itself (1), a pressure source (2), isolation valves (3), and connecting pipeline with a differential barometer (4).

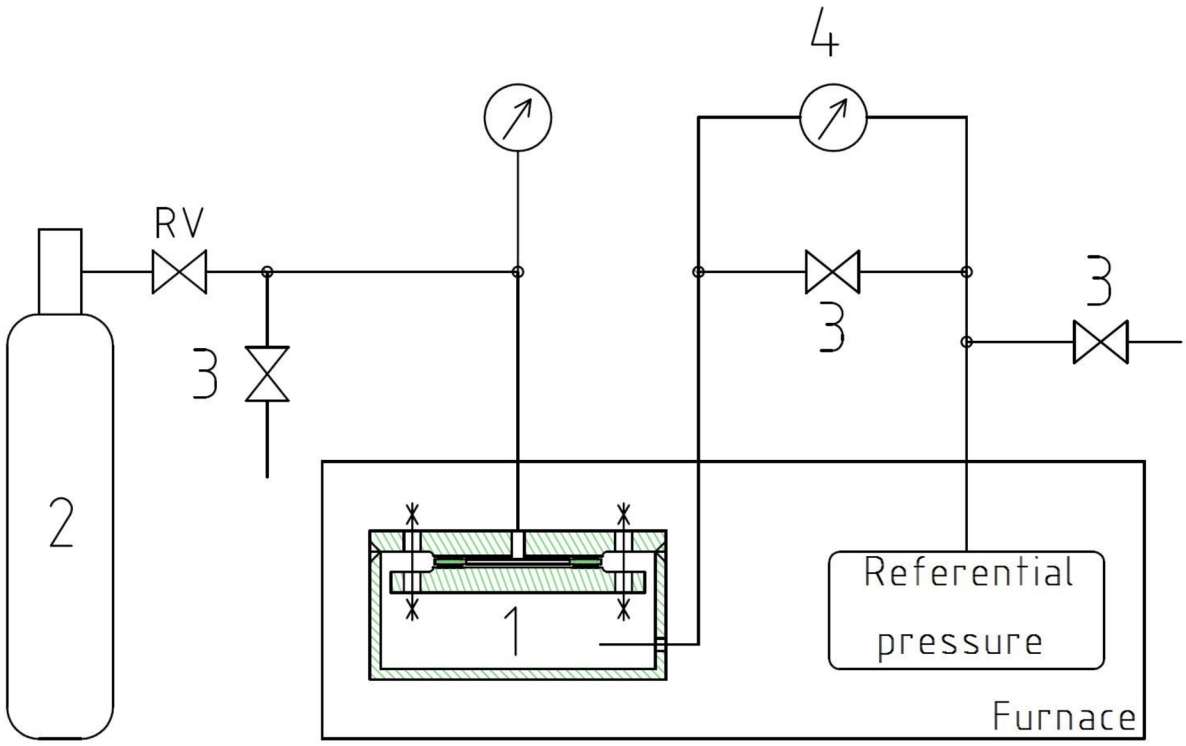

Figure 42: Experimental scheme

5. Conclusion

Material analysis and the assessment of suitability of chosen alloys for the VHTR intermediate heat exchanger flange joint are discussed in the subhead 3.3.

In terms of the experiment the most difficult part would be the flange joint construction. The flange has to be provided with an outer membrane to allow the differential pressure variation measurement. Based to this measurement the leakage rate could be evaluated. The differential pressure measurement is chosen because of the temperature variability and its effects on the pressure. The hermetic closed space has to be reached so that the sealing forces exceed the membrane toughness. This closed space can be reached by welding around the whole diameter of the flange. It is also necessary to avoid or minimize the flange joint force influence. That is why the electron beam welding method (with beam size of 0.5 mm) is chosen for this experiment. Whole experiment is assembled at a room temperature so the negative pressure has to be created to eliminate the thermal pressurizing which cannot be neglected besides high temperature differences. With this experiment the changeability of stainless steel 316 by Inconel 718 in the flange joint application can be assessed. By the end of writing this thesis the Inconel 718 samples have not been available to examine so the electron beam effect had been tested only at the SS316.

BIBLIOGRAPHY

[1] RYSKAMP, J. M. Next Generation Nuclear Plant – High-Level Functions and Requirements [online]. 2003, [cit. 2014-03-05]. URL: https://inlportal.inl.gov/portal/server.pt/document/67962/ineel-ext-03-01163_ngnp_high_lvl_fuct___req_pdf.

[2] VESECKÝ, R., BOUČEK, S. Vysokoteplotní reaktorový systém (VHTR) a jaderná elektrárna příští generace (NGNP). Praha, 14 p. České vysoké učení technické v Praze.

[3] NGNP Alliance. The High Temperature Gas-Cooled ReactorNext Generation Nuclear Energy [online]. [cit. 2014-03-05]. URL: http://www.ngnpalliance.org/images/general_files/HTGR%204%20page%20individual%20040611.pdf.

[4] BEČVÁŘ, J. *Jaderné elektrárny*. 2nd edition, Praha, 1981, 634 p.

[5] CHAPIN, D., et al. The Very High Temperature Reactor: A Technical Summary. 2004.

[6] TRAVIS, B. W., EL-GENK, M. S., 2013, Thermal–hydraulics analyses for 1/6 prismatic VHTR core and fuel element with and without bypass flow. *Energy Conversion and Management*, Vol. 67, p. 325-341.

[7] BILLOT, P., SERAN, J. L., Materials Requirements to Support Research for the Generation IV Systems Development (VHTR, GFR, SFR).

[8] REITSMA, F., Pebble-bed Reactor Core Neutronics Design and Fuel Cycle [online]. 2012, [cit. 2014-03-05]. URL: http://www.iaea.org/NuclearPower/Downloadable/Meetings/2012/2012-10-22-10-26-WS-NPTD/Day-2/8.Reitsma.pdf.

[9] American Nuclear Society, TRISO fuel development progress at INL, ORNL [online]. [cit. 2014-03-05]. URL: https://www.gen-4.org/gif/upload/docs/application/pdf/2014-03/nov13nn_fuel_reprint.pdf.

[10] ZHOU, X., TANG, C., 2011, Current status and future development of coated fuel particles for high temperature gas-cooled reactors, *Progress in Nuclear Energy*, Vol. 53(2), p. 182-188.

[11] SILVA, et al. Shifting study of a VHTR using reprocessed fuel with various TRISO packing fractions. *Nuclear Engineering and Design*. 2012, Vol. 248, p. 42-47

[12] NGNP Alliance, TRISO Fuel News [online]. [cit. 2014-03-05]. URL: http://blog.ngnpalliance.org/triso-fuel-news.

[13] KANG, J.H.,et al. Thermo-mechanical analysis of the prismatic fuel assembly of VHTR in normal operational condition. *Annals of Nuclear Energy*. 2012, Vol. 44, p. 76-86.

[14] DUARTE, J. P., OLIVA, J. d. J. R., Generation IV Nuclear Systems: State of the Art and Current Trends with Emphasis on Safety and Security Features [online]. [cit. 2014-03-05]. URL: http://www.intechopen.com/books/current-research-in-nuclear-reactor-technology-in-

brazil-and-worldwide/generation-iv-nuclear-systems-state-of-the-art-and-current-trends-with-emphasis-on-safety-and-securi.

[15] MILLS, K. C., *Recommended values of thermophysical properties for selected commercial alloys*, Woodhead Publishing Ltd, 2002. 244 p. ISBN 0871707535

[16] MURTY, K., CHARIT, I., Structural materials for Gen-IV nuclear reactors: Challenges and opportunities. *Journal of Nuclear Materials*. 2008, Vol. 383, Num. 1, p. 189-195.

[17] Ústav jaderného výzkumu v Řeži, Superkritická vodní smyčka SCWL.

[18] DOSTÁL, V., Jaderné reaktory IV. generace: Generation IV nuclear reactors. Praha: České vysoké učení technické, 2010, 22 p. ISBN 978-80-01-04678-4.

[19] BUONGIORNO, J., MACDONALD, P. E., Supercritical Water Reactor: Progress Report for the FY-03 Generation-IV R&D Activities for the Development of the SCWR in the U.S. [online]. [cit. 2014-03-05]. URL: http://nuclear.inl.gov/gen4/docs/scwr_annual_progress_report_gen-iv_fy-03.pdf.

[20] ROSENTHAL, M. W., An Account of Oak Ridge National Laboratory's Thirteen Nuclear Reactors [online]. 2009, [cit. 2014-03-05]. URL: http://info.ornl.gov/sites/publications/files/Pub20808.pdf.

[21] Sohal, M. S., et al. *Engineering database of liquid salt thermophysical and thermochemical properties.* 2010, Idaho National Laboratory, Idaho Falls

[22] BARTHOLOMAE, C., Material Selection For Long Term Application in Heat Exchangers in High Temperature Reactors. Hartford, 2010. 40 p. Diploma thesis. University of Hartford, Faculty of Rensselaer Polytechnic Institute.

[23] Special Metals, Inc [online]. 2005, [cit. 2014-03-05]. Monel 400. URL: http://www.specialmetals.com/documents/Monel%20alloy%20400.pdf

[24] Heyman [online]. [cit. 2014-03-05]. Monel. URL: http://www.heyman.cz/media/useruploads/files/cz/technische_angaben/monel.pdf?f=1

[25] Special Metals, Inc [online]. 2007, [cit. 2014-03-05]. Inconel 718. URL: http://www.specialmetals.com/documents/Inconel%20alloy%20718.pdf

[26] Metalworking World. The Hard Task [online]. [cit. 2014-03-05]. URL: http://www2.coromant.sandvik.com/coromant/downloads/articles/aerospace/MWW209_aerospace_The_hard_task.pdf.

[27] Honeywell [online]. 2007, [cit. 2014-03-05]. Airbus A380 Wheels and CARBENIX® Brakes, Advanced braking performance witha lowertotal cost of ownership. URL: http://aerospace.honeywell.com/~/media/UWSAero/common/documents/myaerospacecatalog-documents/ATR_Brochures-documents/A380_Carbenix_Data_Sheet_US.pdf.

[28] SCHOLTZ, R., MATERA, R., Irradiation creep induced stress relaxation of Inconel 718. *Fusion engineering and design.* 200, Vol. 51, p. 165-170.

[29] THOMAS, A., et al. High temperature deformation of Inconel 718. *Journal of materials processing technology*. 2006, Vol. 177, Num. 1, p. 469-472.

[30] OVERFELT, R. A., TAYLOR, R. E., Thermal Conductivity. *Technomic Basel*. 1996, Vol. 23, p. 538-549.

[31] HENDERSON, J. B., STROBEL, A.,Thermal conductivity. *Technomic Basel*. 1996, Vol. 23, p. 530-537.

[32] RICHARDSON, M. J., HAYES, D., MILLS, K. C., MTS Programme on Processability.

[33] Hayes International [online]. 1997, [cit. 2014-03-05]. Hastelloy X Alloy. URL: https://www.haynesintl.com/pdf/h3009.pdf.

[34] TSUJI, H., KONDO, T., Strain-time effects in low-cycle fatigue of nickel-base heat-resistant alloys at high temperature. *Journal of Nuclear Materials*. 1987, Vol. 150, Num. 3, p. 259-265.

[35] NICKEL, H., SCHUBERT, F., SCHUSTER, H., Evaluation of alloys for advanced high-temperature reactor systems. *Nuclear engineering and design*. 1984, Vol. 78, Num. 2, p. 251-265.

[36] KURATA, Y., OGAWA, Y., Internal stress during high-temperature creep of special grade hastelloy X alloys. *Journal of Nuclear Materials*. 1988, Vol. 158, p. 42-48.

[37] TSUJI, H., et al. Applicability of creep damage rules to a nickel-base heat-resistant alloy Hastelloy XR. *Journal of nuclear materials*. 1992, Vol. 199, Num. 1, p. 43-49.

[38] MAGLIC, K. D., PEROVIC, N. L., STANIMIROVIC, A. M., High Temp - High Pressure 25. 1993, p. 429/434.

[39] DUPÁK, L., Mikroobrábění nekovových materiálů elektronovým svazkem. Brno, 2012, 101 p. Diploma thesis. Vysoké učení technické v Brně, Fakulta strojního inženýrství.

[40] GORDINE, J., Some problems in welding Inconel 718. *Welding Journal*. 1971, Vol. 50, Num. 11, p. 480-484.

[41] HUANG, C., et al. A study of the heat-affected zone (HAZ) of an Inconel 718 sheet welded with electron-beam welding (EBW). *Materials Science and Engineering: A*. 2005, Vol. 398, Num. 1, p. 275-281.

LIST OF ABBREVIATIONS AND SYMBOLS

CFD	Computational fluid dynamics
EBW	Electron beam welding
FZ	Fusion zone
GIF	Generation IV international forum
GT-MHR	Gas turbine modular helium reactor
HAZ	Heat affected zone
HTGR	High temperature gas reactor
IHX	Intermediate heat exchanger
LWR	Light water reactor
MSR	Molten salt reactor
ORNL	Oak Ridge National Laboratories
PBMR	Pebble bed modular reactor
SCWR	Supercritical water reactor
SEM	Scanning electron microscope
SS 316	Stainless steel 316
TRISO	Tristructural isotropic
VHTR	Very high temperature reactor

α	Mean coefficient of thermal expansion	$[K^{-1}]$
ε	Elongation	[%]
λ	Thermal conductivity	$[W \cdot m^{-1} \cdot K^{-1}]$
ν	Poisson's ratio	[-]
ρ	Density	$[kg \cdot m^{-3}]$
σ_c	Comprehensive strength	[MPa]
σ_t	Tensile strength	[MPa]
$\sigma_{1,2}$	Nominal stress	[MPa]
C_p	Heat capacity	$[J \cdot g^{-1} \cdot K^{-1}]$
E	Young's modulus	[GPa]
$t_{1,2}$	Time to rupture	[hr]

LIST OF FIGURES

LIST OF TABLES